Alkali-calcic and alkaline post-orogenic (PO) granite magmatism: Petrologic constraints and geodynamic settings

ARTICLE *in* LITHOS · DECEMBER 1998

Impact Factor: 4.48 · DOI: 10.1016/S0024-4937(98)00025-5

8 AUTHORS, INCLUDING:

Bernard Bonin
Université Paris-Sud 11

Francois Bussy
University of Lausanne

Lithos 45 (1998) 45–70

Alkali-calcic and alkaline post-orogenic (PO) granite magmatism: petrologic constraints and geodynamic settings

Bernard Bonin [a,*], Abla Azzouni-Sekkal [b], François Bussy [c], Sandrine Ferrag [a,b]

[a] *Département des Sciences de la Terre, CNRS-ERS 388, Bâtiment 504, Université de Paris-Sud, F-91405 Orsay Cedex, France*
[b] *Laboratoire de Pétrologie-Structurologie, Institut des Sciences de la Terre, UST-HB, BP 32, El Alia 16111 Bab Ezzouar, Algiers, Algeria*
[c] *Institut de Minéralogie et Pétrographie, BFSH2, Université de Lausanne, CH-1015 Lausanne-Dorigny, Switzerland*

Received 8 January 1998; accepted 26 June 1998

Abstract

The end of an orogenic Wilson cycle corresponds to amalgamation of terranes into a Pangaea and is marked by widespread magmatism dominated by granitoids. The post-collision event starts with magmatic processes still influenced by subducted crustal materials. The dominantly calc-alkaline suites show a shift from normal to high-K to very high-K associations. Source regions are composed of depleted and later enriched orogenic subcontinental lithospheric mantle, affected by dehydration melting and generating more and more K- and LILE-rich magmas. In the vicinity of intra-crustal magma chambers, anatexis by incongruent melting of hydrous minerals may generate peraluminous granitoids bearing mafic enclaves. The post-collision event ends with emplacement of bimodal post-orogenic (PO) suites along transcurrent fault zones. Two suites are defined, (i) the alkali-calcic monzonite–monzogranite–syenogranite–alkali feldspar granite association characterised by [biotite + plagioclase] fractionation and moderate [LILE + HFSE] enrichments and (ii) the alkaline monzonite–syenite–alkali feldspar granite association characterised by [amphibole + alkali feldspar] fractionation and displaying two evolutionary trends, one peralkaline with sodic mafic mineralogy and higher enrichments in HFSE than in LILE, and the other aluminous biotite-bearing marked by HFSE depletion relative to LILE due to accessory mineral precipitation. Alkali-calcic and alkaline suites differ essentially in the amounts of water present within intra-crustal magma chambers, promoting crystallisation of various mineral assemblages. The ultimate enriched and not depleted mantle source is identical for the two PO suites. The more primitive LILE and HFSE-rich source rapidly replaces the older orogenic mantle source during lithosphere delamination and becomes progressively the thermal boundary layer of the new lithosphere. Present rock compositions are a mixture of major mantle contribution and various crustal components carried by F-rich aqueous fluids circulating within convective cells created around magma chambers. In favourable areas, PO suites pre-date a new orogenic Wilson cycle. © 1998 Elsevier Science B.V. All rights reserved.

Keywords: Post-orogenic; Granitoids; Alkaline; Alkali-calcic; Mantle; Crust; Fluids; Fractionation

* Corresponding author. Tel.: +33-1-69-15-67-66; Fax: +33-1-69-15-67-72; E-mail: bbonin@geol.u-psud.fr

PII: S0024-4937(98)00025-5

1. Post collision granites suites: a case of multi-source multi-process magmatism

The orogenic Wilson cycle evolves from the break up of an older Pangaea through oceanic basin opening and closure to accretion of displaced terranes into a younger Pangaea (Dewey, 1988). Three major episodes can be identified. The first episode, intra-continental rifting characterised by plate divergence, is followed by oceanic basin opening and ends with the onset of subduction along active margins. The second episode resulting from plate convergence is dominated by ocean–ocean and/or ocean–continent subduction, oceanic basin closure and continent–continent collision, and associated with wrench and thrust tectonics. The dominantly ensialic third episode consists of accretion of continental blocks or terranes by 'docking' and/or hyper-collision with uplift and transcurrent fault tectonics generating transpressional and transtensional regimes. The geodynamic settings of the three distinct episodes are essentially governed by lithosphere and asthenosphere rheologies (see Black and Liégeois, 1993, and references therein).

Regarding the third episode of syn- to post-collision, Black and Liégeois (1993) distinguish mantle delamination followed by lithosphere growth (stages C and D, Fig. 4, p. 92). The orogenic continental lithosphere is composed of a thickened crust and a thinned upper mantle and overlies an asthenosphere still affected by oceanic and continental subduction products. During stage C thermal instability and weak links with the crust cause lithosphere thinning by delamination. Upwelling of hot asthenosphere induces magmatic under-plating, low-pressure high-temperature metamorphism, partial melting of lower crust and rapid uplift due to isostasy. This leads to juxtaposition of a cratonic foreland with cold crust and thick lithosphere and orogenic belts with hotter crust and thin lithosphere. Eventually, during stage D the lithospheric mantle of former mobile belts experiences progressive growth with time by cooling and basal accretion of deeper materials, as long as quiet conditions prevail. If not, cratonisation effects are destroyed and continental break up parallel to ancient orogenic belts (Vauchez et al., 1997) starts a new Wilson cycle.

Magmatic rocks found in orogenic belts provide a record of the thermal and chemical evolution of deep lithospheric roots of the developing orogen. Though the rocks eventually sampled may be the end product of several generative processes, magmatic suites can be discriminated on the basis of geological, mineralogical and chemical characteristics (Barbarin, 1990; Lameyre and Bonin, 1993). Distinct suites associated with the successive episodes of a Wilson cycle reflect a relation between geodynamic factors and magma types, which constitutes the basis of the tectonic discrimination schemes currently used (e.g., Pearce et al., 1984; Maniar and Piccoli, 1989).

After collision, magmatic suites are located principally within mobile belts where reactivated pre-existing zones of weakness control their emplacement during ensialic deformation. They change abruptly from typically orogenic syn- to post-collision suites emplaced during collision, uplift and subsequent gravitational collapse of the hot and thick crust to post- to non-orogenic suites related to transcurrent faulting, peneplanation and the development of fault-controlled intra-continental molassic basins (Bonin, 1990; Turner et al., 1992). The aim of this paper is to focus on the nature, sources and differentiation processes of post- to non-orogenic suites emplaced during the stage D of Black and Liégeois (1993). Two world-wide orogenic cycles will be examined: (i) the Late Proterozoic event with examples from Africa and Brazil and (ii) the Late Palaeozoic event with examples from Europe and the Western Mediterranean area.

1.1. Nomenclature aspects

Collision corresponds to the welding of at least two terranes into a new continental land. The subsequent episodes can be considered as intra-continental and different terms should be explained.

'Post-collision' stands for the episode occurring after the major collision episode. Continuing plate convergence result in intra-continental thrust and wrench deformation and/or lateral escape of discrete terranes. This episode can be considered also as 'late orogenic'. Magmatic events encompass anatectic peraluminous S-type granite suites of main crustal origin and high to very high-K calc-alkaline suites with an orogenic depleted/enriched subcontinental lithospheric source (McKenzie and O'Nions, 1995) akin to the source of the previous orogenic pre-collision calc-alkaline suites.

'Post-orogenic (PO)' stands for the subsequent episode, when the geodynamic context becomes entirely intraplate, with the welded terranes moving according to the same pole of rotation. Magmatic suites are emplaced along shear zones in transcurrent tectonic regimes and display markedly alkaline affinities with a new undepleted and enriched mantle source.

'Anorogenic' is synonymous with 'non-orogenic' and stands for later episodes. Alkaline magmatic suites characterised by the same mantle source are emplaced along intraplate rifts. No association with local plate convergence is evidenced, though a relation with contemporaneous global scale collision events can be evidenced (Black et al., 1985).

'Post-tectonic' and 'atectonic' are irrelevant terms for magmatic activity, as demonstrated by abundant field evidence on the 'room problem' and volumes necessitated by magma circulation.

2. Late Proterozoic PO granite suites

A Neoproterozoic (750–550 Ma) major orogenic event is recorded in almost all the continental pieces of Gondwana (e.g., Pan-African in Africa, Kennedy, 1964; Brasiliano in the Brazilian shield, Almeida et al., 1981; Cadomian in the Armorican Massif of France and surrounding areas, D'Lemos et al., 1990). Kennedy (1964) defines the Pan-African as a thermo-tectonic event resetting isotopic dates at ca. 500 Ma, except for smaller cratonic areas still retaining older Archaean and Palaeoproterozoic ages. Occurrences of true ophiolites, juvenile island arc assemblages and continental scale collisions provide convincing evidence for plate tectonics (Black et al., 1979). Considered together with its extensions in other continents, such as the Brasiliano belt of South America and the Cadomian terrane of Europe, the Pan-African orogen is comparable in scale to the currently active Alpine–Himalayan–Circum Pacific belt.

The Trans-Saharan belt of northern Africa extends from Mali to Saudi Arabia and comprises numerous accreted island arcs and reactivated Archaean and Palaeoproterozoic continental blocks. Up to 23 displaced terranes were accreted during the Pan-African episodes along major north–south-oriented shear zones (Fig. 1) and formed ultimately the Tuareg shield (Black et al., 1994). Its southern extension along the Atlantic coast of Brazil and Uruguay resulted from the amalgamation of discrete terranes, the easternmost ones corresponding to accreted juvenile arcs and the westernmost ones to a collage of older continental slices (Caby, 1989). The belt is characterised by voluminous Late Proterozoic orogenic suites, with tonalite–trondhjemite–granodiorite associations within island-arc assemblages and normal to high-K calc-alkaline batholiths elsewhere, pre-Ordovician molassic intra-continental basins (Fabre, 1988) and widespread Phanerozoic anorogenic alkaline magmatism (Black et al., 1985). Attention will be focused on three PO suites: (i) the 'Taourirt' suite of Hoggar, Algeria, (ii) the province of Adrar des Iforas, Mali, and (iii) the suite of Saibro, southern Brazil.

2.1. The 'Taourirt' suite of Hoggar, Algeria

The Hoggar, Algeria, constitutes the central part of the Trans-Saharan belt and results from the welding of ophiolite-bearing juvenile terranes onto strongly reworked older terranes. More than 20 PO granite centres form a cluster of zoned plutons within an elongated 250×70 km igneous province and constitute the 'Taourirt' suite, the local word 'Taourirt' defining an isolated mountain clearly visible in the distance. They were emplaced within thrust and shear zones related to terrane boundaries between In-Tedeini (It), Iskel (Isk) and Laouni (La) (Fig. 2). Most centres are located along faults bordering Iskel and within it. Centres within Laouni mark out faults related to the huge north–south-trending 750 km-long 4°50′E shear zone.

Neoproterozoic country rocks comprise the shelf-type and volcano-sedimentary Lower Pharusian Supergroup and the volcanic and volcano-clastic Upper Pharusian Supergroup. The so-called 'Pharusian unconformity' represent a cryptic suture with occurrences of eclogite lenses (Bertrand et al., 1986). Two groups of syn-orogenic batholiths are distinguished: the older is exposed in Iskel only, with 870 Ma calc-alkaline Cordilleran-type diorite–granodiorite and 840 Ma anatectic K-feldspar megacrystic gran-

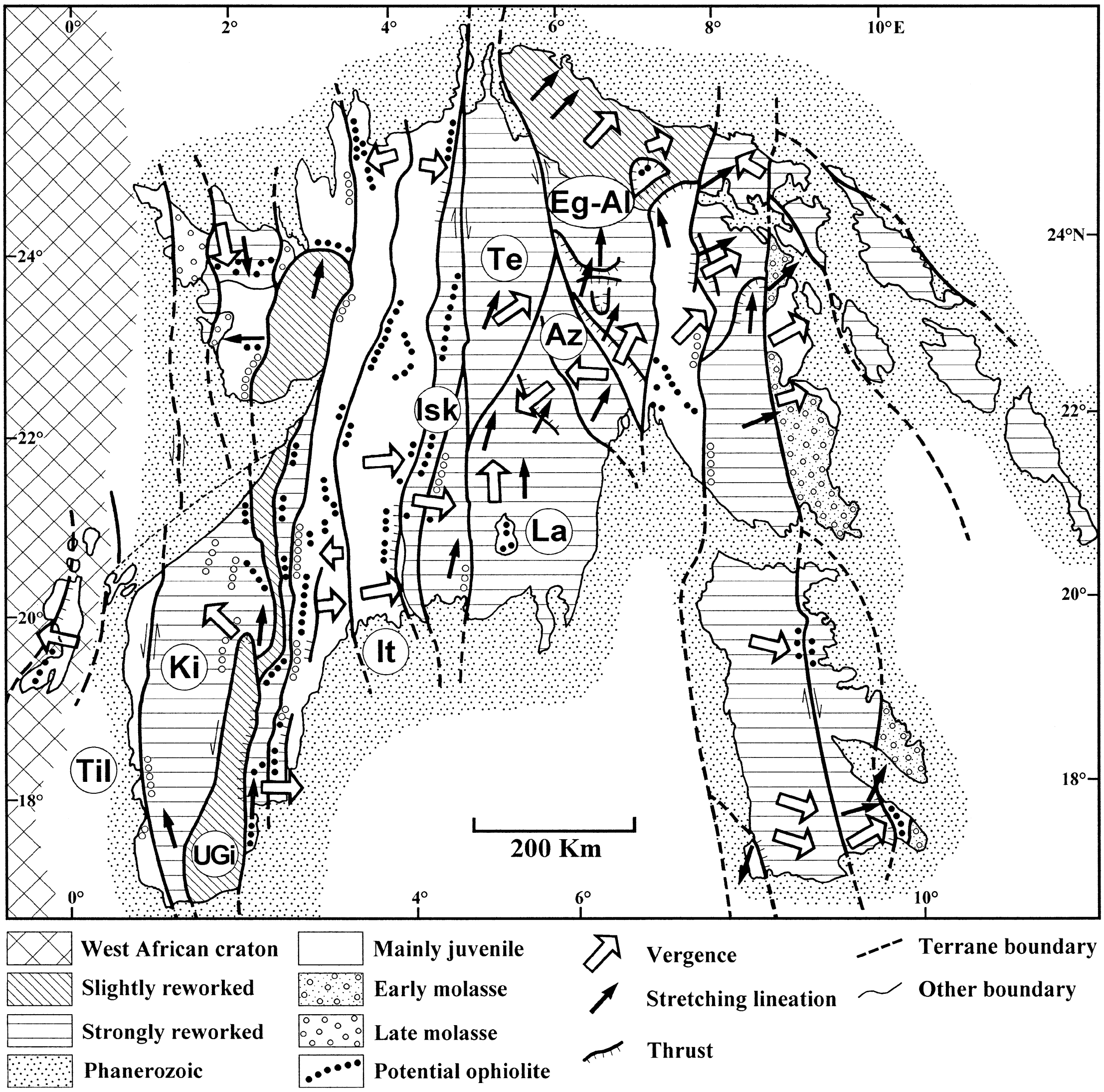

Fig. 1. Black et al. (1994) reconstruction of the Tuareg shield. Solid arrows indicate movement directions determined from field and laboratory works. Double dashed line is the eastern boundary of the West African craton deduced from gravity anomalies. Abbreviations of terranes discussed in the text: Adrar des Iforas, Mali: Til. Tilemsi, Ki. Kidal, Ugi. Iforas granulitic unit; Hoggar, Algeria: It. In-Tedeini, Isk. Iskel, La. Laouni, Te. Tefedest, Eg-Al. Egéré-Aleksod, Az. Azrou-n-Fad.

ite; the younger is widespread elsewhere with 730–700 Ma volcanic arc assemblages and 650–570 Ma normal to high-K calc-alkaline batholiths and anatectic potassic granite (Black et al., 1994, and references therein).

The 'Taourirt' suite intrudes the different Pharusian units and two centres are covered by Ordovician sandstone (Fabre, 1988). Rb–Sr, K–Ar and ^{40}Ar–^{39}Ar determinations centred around 570–520 Ma (Cahen et al., 1984; Cheilletz et al., 1993; Zaimen et al., 1994; works in progress). The 'Taourirt' suite is dominantly granitic, with scarce basic to intermediate rocks, and four major rock types are defined: G I monzogranite, G IIa monzogranite and syenogranite,

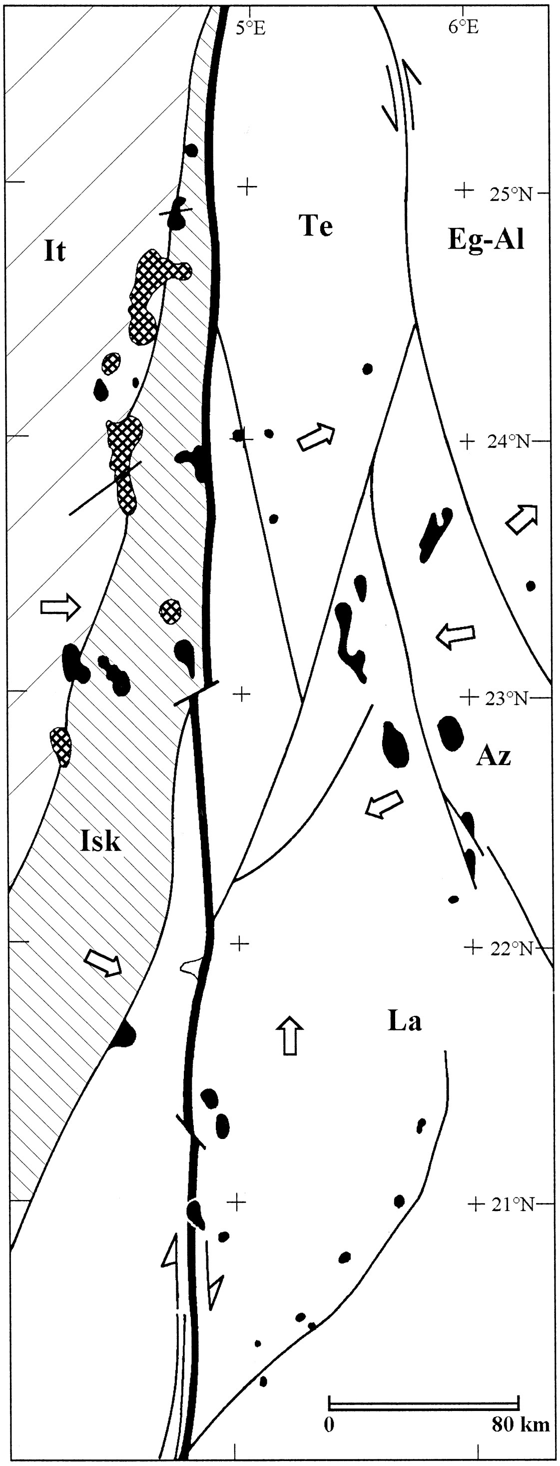

G IIb alaskite (alkali feldspar granite) and G III alkali feldspar syenite and granite (Table 1).

G I monzogranite is present in a small number of complexes. ΣREE contents average 200 ppm, with patterns yielding moderate fractionation, slight LREE enrichment and weak negative Eu anomalies. G IIa monzogranite and syenogranite are exposed in almost all complexes studied. The rock-forming mineralogy is the same as within G I monzogranite, with K-feldspar being more abundant than plagioclase. The accessory paragenesis is similar, with addition of thorite + fergusonite + monazite + xenotime. ΣREE contents average 250 ppm, with less fractionated patterns and more pronounced negative Eu anomalies. G IIb alaskite (alkali feldspar granite) is the most evolved type of the suite characterised by pure albite and Li-bearing mica (protolithionite to zinnwaldite). Extremely high SiO_2 contents contrast with extremely low Ti, Mg, Ca and P contents. REE patterns show little or no fractionation and deep negative Eu anomalies. Tetrad effects on La–Ce–Pr–Nd and Gd–Tb–Dy–Ho suites of lanthanide elements (Bau, 1996) result in gull wing-shaped patterns with downward concavity. With the lowest abundances of Sr, Ba, LREE, Zr and the highest abundances of Rb, U, Th, Nb, Y, MREE, HREE alaskite exhibits the features defining the low-*P* subtype of topaz granite (Taylor, 1992).

The G III association is exposed in a small number of complexes. Mesoperthitic alkali feldspar is the

Fig. 2. Geological setting of the 'Taourirt' suite (Azzouni-Sekkal and Bonin, 1998). Complexes studied in crosses, others in black. Abbreviations and lithology of the displaced terranes: It, In-Tedeini: greenschist facies greywacke, volcanic and clastic rocks, calc-alkaline granitoids (650–550 Ma); Isk, Iskel: greenschist facies platform sedimentary rocks, mafic–ultramafic sills, calc-alkaline granitoids (870 Ma), high-K granite and syenite (840 Ma) and volcaniclastic sequences; La, Laouni: amphibolite facies basement gneiss and several supracrustal sequences, greenschist facies shelf sedimentary rocks, anatectic potassic granite, PO Sn–W-bearing topaz granite (540–520 Ma); Te, Tefedest: amphibolite facies basement gneiss and several supracrustal sequences, calc-alkaline granitoids; Eg-Al, Egéré-Aleksod: Archaean and Eburnean granulitic gneiss, supracrustal banded iron formation, Pan-African high-*P* amphibolite facies gneiss with eclogite, foliated granodiorite, no huge calc-alkaline batholiths; Az, Azrou-n-Fad: similar to Eg-Al terrane.

Table 1
The 'Taourirt' suite of Hoggar, Algeria

Rock types		gabbro and diorite (stocks, enclaves) G I monzogranite G IIa monzogranite and syenogranite G IIb alaskite (alkali feldspar granite) G III alkali feldspar syenite and granite	
Rock-forming mineralogy		G I quartz + K-feldspar + plagioclase + edenite–hornblende + biotite G IIa quartz + K-feldspar + plagioclase + biotite ± hornblende G IIb quartz + K-feldspar + albite + protolithionite–zinnwaldite G III alkali feldspar ± quartz ± plagioclase + hedenbergite + hastingsite–hornblende + biotite ± grünerite ± riebeckite	
Accessory mineralogy		G I zircon + allanite + titanite + ilmenite + magnetite + apatite G IIa zircon + allanite + titanite + ilmenite + magnetite + apatite + thorite + fergusonite + monazite + xenotime G IIb zircon + allanite + titanite + fluorite + topaz ± tourmaline ± garnet G III zircon + thorite + allanite + chevkinite + ilmenite + magnetite + apatite + fluorite	
Major element chemistry	SiO_2	G I 69–73 wt.% G IIa 70–76.5 wt.% G IIb ≤ 78 wt.% G III 65–69 and 73–77 wt.%	
	CaO	G I 1.2–2.2 wt.% G IIa 0.8–1.8 wt.% G IIb < 0.02 wt.% G III 2–2.5 and 0.5–0.9 wt.%	
	ASI	G I metaluminous G IIa metaluminous G IIb peraluminous G III metaluminous to peralkaline	
	alkali-calcic	G I, G IIa, G IIb	
	alkaline	G III	
Trace elements (ppm)	Rb	200–410 (G I, G IIa, G IIb)	120–260 (G III)
	Ba	14–800	37–600
	Th	20–85	15–60
	Zr	65–300	180–1200
	Y	22–140	40–60
REE patterns	La (ppm)	10–80	35–280
	$(La/Yb)_N$	0.6–10	13–30
	Eu/Eu*	0.02–0.75	0.04–0.16
		gull wing shape tetrad effects in G IIb only	gull wing shape no tetrad effects
Isotope ratios	Sri	0.706–0.723	
Age of emplacement		570–520 Ma	

Refs. Azzouni-Sekkal and Boissonnas (1993), Cheilletz et al. (1993), Zaimen et al. (1994), Azzouni-Sekkal and Bonin (1998), works in progress.

chief mineral component. The compositionally expanded group comprises metaluminous to peralkaline alkali feldspar syenite and granite. ΣREE contents are higher in syenite (1100 ppm) than in granite (200–400 ppm). Fractionated and gull wing-shaped REE patterns show LREE enrichment, pronounced negative Eu anomalies, no tetrad effects and upward concavity. Ba and Sr levels are intermediate between PO and early anorogenic types of alkaline granitoids (Bonin, 1990).

Two distinct suites are evidenced. The major one, composed of G I, G IIa and G IIb, is alkali-calcic in the sense of Peacock (1931). Azzouni-Sekkal and Boissonnas (1993) calculate a liquid line of descent by extraction of leucocratic [plagioclase + K-feldspar + biotite ± amphibole + allanite + titanite] monzo-syenitic assemblages. The markedly alkaline G III types follow a different trend. The two associations were emplaced synchronously in the complexes where they occur together. Azzouni-Sekkal and Boissonnas (1993) interpret them as the transition from late-orogenic calc-alkaline to non-orogenic alkaline magmatism implying increasing mantle involvement.

2.2. The alkaline province of Adrar des Iforas, Mali

The Adrar des Iforas, Mali, constitutes the southwestern appendix of the Tuareg shield in the Trans-Saharan belt of northern Africa. Like the Hoggar it resulted from a collage of several displaced terranes (Fig. 1), namely from west to east, Tilemsi (Til) with juvenile island-arc assemblages, Kidal (Ki) with Proterozoic supracrustal formations, and Iforas granulitic unit (Ugi) with 2.1 Ga granulites.

Kidal is characterised by the high-grade so-called Kidal Assemblage comprising old granulitic gneisses, Palaeo- to Neoproterozoic metasedimentary lenses and abundant pre-tectonic intrusives. During the major Pan-African event it was cross-cut by successive intrusive suites (Liégeois et al., 1987). The syn-subduction episode is characterised by volcano-clastic and volcanic deposits with scarce large Cordilleran-type plutons displaying a low-K to normal calc-alkaline trend. The only dated intrusion is the 695 Ma Teggart quartz diorite. By contrast the syn-collision episode is well represented by the huge 300 km × 50 km late tectonic Adrar des Iforas batholith which follows a high-K calc-alkaline trend. Syn-kinematic plutons were deformed during their crystallisation. Ages of emplacement are bracketed by isotopic dates of 615 and 580 Ma indicating a short-lived episode. Rb–Sr systematics of earlier magmatic units were also reset at 600 Ma representing, therefore, the climax of the collision event. Late tectonic magmatism, with Rb–Sr dates clustered in the 575–545 Ma range, comprises the Yenchichi 2-type syenogranite plutons and the dense WNW-ESE Telabit, Dohendal and Yenchichi dyke swarms, which provide the reference for sliding normalisation (Liégeois et al., 1998).

After emplacement of WNW-ESE dyke swarms the PO 560–540 Ma alkaline group was emplaced in three diachronous episodes, (i) Tahrmert peralkaline granite, (ii) N–S dyke swarms acting as feeding conduits for Tiralrar thick ignimbritic rhyolite sheets and (iii) subvolcanic ring complexes in which syenites and granites define two evolutionary trends. The onset of alkaline magmatism was induced by reactivation of N–S shear zones around 550 Ma (Yenchichi mylonites) related to reversal of the sense of movement (‘harpoon effect’, Black et al., 1985). Metaluminous amphibole–biotite hypersolvus granites and peraluminous biotite subsolvus granites constitute the aluminous trend, the peralkaline trend comprises metaluminous fayalite–pyroxene–amphibole hypersolvus granites and peralkaline aenigmatite–aegirine–arfvedsonite hypersolvus granites (for characteristics, see Liégeois and Black, 1987).

Post-collision high-K calc-alkaline and PO alkaline groups yield indistinguishable dates but slightly different isotope ratios. Sr–Nd–Pb–O isotopes systematics preclude any direct derivation from old crustal units and Liégeois (1988) suggests two contrasting sources, subduction-related depleted mantle for the post-collision high-K calc-alkaline suites and more primitive mantle with possible DUPAL signature for the PO alkaline suite.

2.3. The Saibro intrusive suite, southern Brazil

The Sul-rio-grandense shield, a small piece of the Brasiliano belt of the western Atlantic coast, occurs in southern Brazil and Uruguay and is made up of Proterozoic metamorphic assemblages intruded by numerous granitoids and overlain unconformably by volcano-sedimentary formations. The shield is subdivided into two contrasting zones, eastern and western.

The eastern zone is composed mainly of juvenile volcanic arc formations. On the basis of field evidence and Rb–Sr data, the progressive maturing of the arc is substantiated by successive igneous suites (Frantz and Nardi, 1992). Arc assemblages were affected by a major 885 Ma compressional event reaching amphibolite facies and intruded by phase-1 syn-thrust 830 Ma low-K calc-alkaline tonalite–trondhjemite–granodiorite Piratini gneisses. This ensemble was affected by low-*P* high-*T* metamorphism inducing anatexis, migmatites and cordierite-bearing S-type granodiorite, carrying crustal xenoliths and spinel–sillimanite–cordierite restites. The phase-2 syn-shear 775 Ma high-K calc-alkaline granodiorite–monzogranite Pinheiro Machado suite was related to transcurrent movement along narrow shear zones and the development of greenschist facies. The two magmatic phases lasted about 60 Ma. They correspond approximately to the episodes affecting the Iskel terrane of Hoggar and predate the major Brasiliano episode by 100 Ma.

At the boundary between western and eastern zones the Cordilhera peraluminous suite comprises

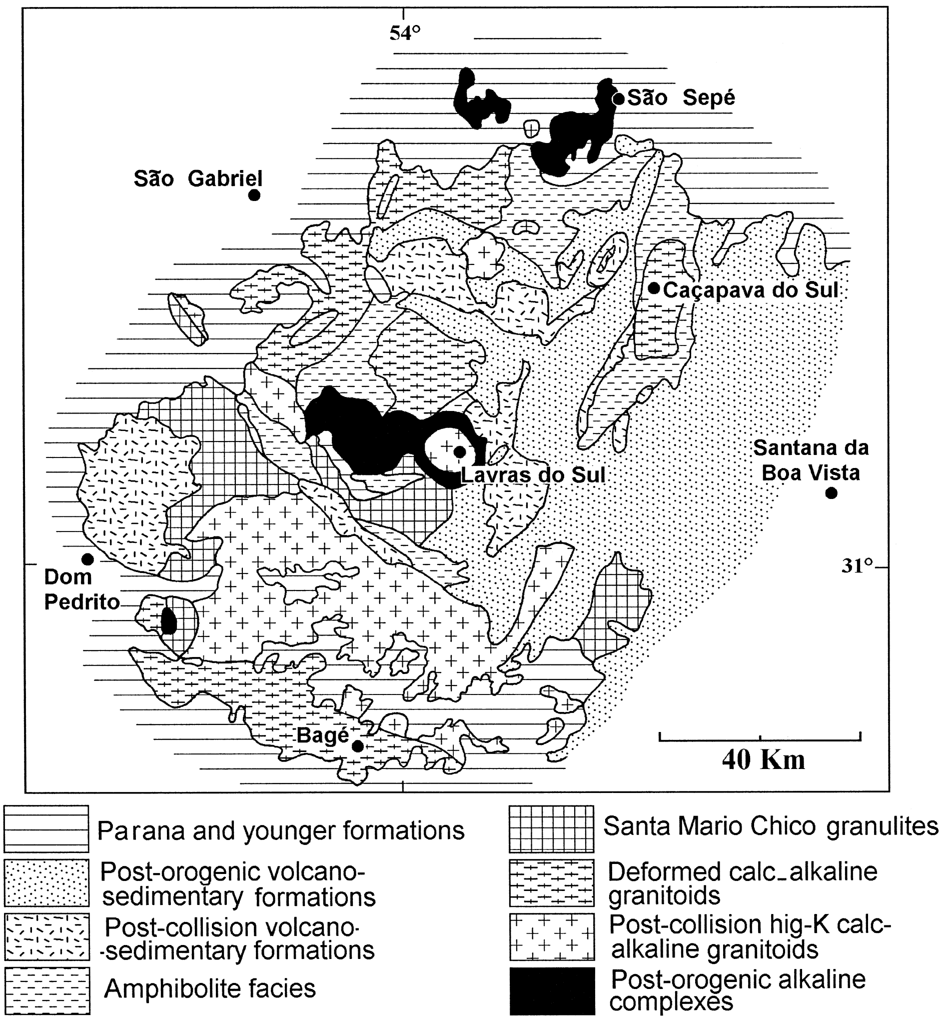

Fig. 3. The Sul-rio-grandense shield (Bitencourt et al., 1987; Nardi and Bonin, 1991).

two-mica leucogranite and garnet–tourmaline muscovite leucogranite (Nardi and Frantz, 1995). Like the phase-2 calc-alkaline suite, syn to late-kinematic emplacement within shear zones along a NE-trending system was accompanied by greenschist facies metamorphism of the country rocks. The Cordilhera suite resembles the Variscan peraluminous suite of Europe as emphasised by occurrences of greisens, tourmalinites, beryl pegmatites and Sn–W mineralisations.

The western zone (Fig. 3) is a more complex continental terrane and results from the stacking and piling of tectonic slices, with the Santa Maria Chico 2.0 Ga granulite complex as the oldest and uppermost unit and the Passo Feio amphibolite complex as the lowermost unit. The tectonic slices are cross-cut by intrusive suites and overlain by volcano-sedimentary units. Different dates correspond to distinct phases (Bitencourt et al., 1987). The phase-1 syn-thrust 660 Ma granodiorite–monzogranite calc-alkaline suite is composed by orthogneisses related to amphibolite facies metamorphism and planar deformation. The phase-2 syn-shear 640–610 Ma shoshonitic association comprises the K-feldspar megacrystic monzodiorite to monzogranite Lavras do Sul suite and volcanic-pyroclastic formations (Nardi and Lima, 1985) unrelated to metamorphic events and emplaced under post-collision tensional regimes. The orogenic magmatic phases have lasted again about 100 Ma and correspond to the major Brasiliano episode. There is one exception to this general scheme. In the Passo Feio lowermost unit the normal calc-alkaline granodiorite to syenogranite Caçapava do Sul suite displays flat foliation planes and N10°-trending mineral lineations related to amphibolite to greenschist facies in country rocks, like the 660 Ma syn-thrust phase-1 suite. The unexpectedly younger Rb–Sr date of 550 Ma (Nardi and Bitencourt, 1989) needs further refinement.

In every zone of the shield, magmatic activity ended with the PO phase-3 alkaline suite which was given various local names, Saibro in western zone, Dom Feliciano in eastern zone and Encruzilhada do Sul in boundary zone. Strike-slip movements along

Table 2
The Saibro intrusive suite of southern Brazil

Rock types		syenite hornblende–biotite hypersolvus granite arfvedsonite–aegirine granite hornblende–biotite subsolvus granite	
Rock-forming mineralogy		metaluminous to peraluminous: quartz + alkali feldspar ± plagioclase + edenite–hornblende + biotite ± clinopyroxene peralkaline: quartz + alkali feldspar + arfvedsonite + aegirine	
Accessory mineralogy		zircon + allanite + titanite + ilmenite + magnetite + apatite + fluorite ± carbonates	
Major element	SiO_2	54–66 and 70–77 wt.%	
Chemistry	CaO	1.2–6.8 and 0.2–0.7 wt.%	
	ASI	metaluminous, slightly peraluminous and peralkaline alkaline suite	
Trace elements (ppm)	Rb	150–200	
	Ba	40–800	
	Zr	170–750	
	Y	35–75	
REE patterns	La (ppm)	27–76	
	$(La/Yb)_N$	4–20	
	Eu/Eu*	0.05–1.0	
		gull wing shape, no tetrad effects	
Isotope ratios	Sri	0.703–0.705	0.707–0.711
Age of emplacement		575 and 550–540 Ma	460–450 Ma (?)

Refs. Nardi and Bonin (1991), Frantz and Nardi (1992).

shear zones controlled the emplacement. Isotopic dates are identical throughout the shield, ranging from 575 Ma for Piquiri syenite to 550–540 Ma for most granites. The phase-3 alkaline suite post-dates the orogenic phase-1 and phase-2 magmatic episodes by about 100 Ma in the western zone and at least 200 Ma in the eastern zone of the shield. Younger 460–450 Ma Rb–Sr dates have been determined in Ramada subsolvus granite and some dyke swarms. The apparent time lag of 80 Ma is difficult to reconcile with other data and, according to field evidence (miarolitic cavities, late oxidation effects, active faults), could be ascribed to resetting by fluids percolating along shear zones.

The alkaline suite is compositionally expanded (Table 2) with rare syenites, abundant granites and associated volcanic rocks. Two evolutionary trends are defined. The aluminous trend comprises metaluminous hypersolvus and mildly peraluminous subsolvus granites. The peralkaline trend of hypersolvus granites is less represented. Thick trachyte–rhyolite ignimbritic sheets covering vast areas within and around red molasse basins and associated hypabyssal dyke swarms constitute the volcanic association. HFSE are relatively depleted in biotite-bearing granites, while HREE, Zr and Y contents increase sharply in the peralkaline trend. ΣREE contents are higher in amphibole-bearing granites (230–340 ppm), lower in biotite-bearing granite (120-210 ppm). Slightly fractionated and gull wing-shaped REE patterns yield LREE enrichment, variably negative Eu anomalies, no tetrad effects and upward concavity. Ba and Sr levels correspond to the PO type of alkaline granitoids (Bonin, 1990). On the basis of Piquiri field evidence, where alkaline granite is closely related to biotite-bearing pyroxene–amphibole layered syenite, Nardi and Bonin (1991) calculates a liquid line of descent by extraction of a leucocratic [plagioclase + K-feldspar + amphibole + Fe–Ti oxides + apatite $\pm$ REE-rich accessory minerals] syenitic assemblage.

3. Late Palaeozoic post-Variscan granite suites

Successive Palaeozoic orogenic events were responsible for progressive welding of almost all continental terranes into the last Pangaea present at the Earth's surface. Amalgamation was completed at the end of the Carboniferous before onset of continental break-up during the Permian. The different episodes were given different names, the first being the ca. 400 Ma Caledonian, followed by the ca. 350 Ma Variscan and, ultimately, the ca. 300 Ma Alleghanian. The names were defined originally on a regional basis, e.g., Caledonian for the orogenic belt extending from Ireland and Scotland toward Scandinavia and Greenland, and should not be used in other areas. However, the common usage that has prevailed is based mainly on age grounds, e.g., Caledonian for Lower Palaeozoic orogenic events.

The Variscan belt is a large orogen extending over 8000 km from the Appalachians in North America to the Bohemian massif in central Europe. It results from the complex, mainly collisional interactions of two super-continents, Laurasia to the north and Gondwana to the south. The scattered occurrence of Cadomian ages in south Europe and eastern North America is interpreted as evidence of Gondwana-derived microcontinents, such as Avalon, Armorica, Iberia, extending to the north as far as the Elbe valley (Wenzel et al., 1993), that collided with the Laurasia megacontinent (Ziegler, 1986). Schaltegger (1994) concludes tentatively that the Helvetic realm and the European foreland of the Alpine belt were consolidated within the present configuration before Caledonian and Variscan events. Attention will be focused on two PO suites post-dating Upper Palaeozoic orogenic events in the Alpine belt (Bonin et al., 1993; Bonin, 1997), (i) the 300-Ma Mont-Blanc–Aar–Gotthard suite, Western and Central Alps, emplaced after the end of the Variscan event, and (ii) the Permo-Triassic Western Mediterranean alkaline province, emplaced after the very end of orogenic events and considered as either post-Variscan/Alleghanian, or eo-Alpine, or both.

3.1. The 300-Ma Mont-Blanc–Aar–Gotthard suite, Western and Central Alps

In western-central Europe the Variscan belt was subsequently reworked by the Tertiary Alpine orogeny. As a consequence the best exposed outcrops of Variscan rocks are located in the weakly overprinted outer zone of the Alpine arc, i.e., the so-called 'External Crystalline Massifs' of the French and Swiss Alps, such as Mont-Blanc, Aiguilles-

Rouges, Aar and Gotthard massifs (Fig. 4). All four massifs consist of a complex assemblage of tectonic units composed of partly migmatised ortho- and paragneisses, interlayered volcanics, mafic–ultramafic lenses and granitic plutons. This assemblage, reminiscent of a metamorphosed accretionary prism, probably resulted from large-scale thrust and transcurrent fault tectonics linked to oblique accretion of terranes or continental blocks by docking and/or hypercollision.

Oceanic crust subduction during the Ordovician is documented in Gotthard massif by island arc-type eclogitised metagabbros, dated at 467–475 Ma (zircon, Oberli et al., 1994), in Aiguilles-Rouges and Mont-Blanc massifs by MORB-like retro-eclogites with a magmatic age of 453 Ma (zircon, Paquette et al., 1989) and by several volcanic arc-type calc-alkaline orthogneisses dated at around 455 Ma (Bussy and von Raumer, 1993).

Continent–continent or continent–[island-arc + accretionary prism] collision started during the Devonian and led to major crustal thickening. Barrowian-type metamorphism subsequently developed in mid-crustal levels and is dated at 327 Ma (monazite from high-T metapelites in Aiguilles-Rouges massif, Bussy and Hernandez, 1997) and at 330 Ma (zircon and rutile from metagraywackes in Aar massif, Schaltegger, 1994). Oblique compression generated transcurrent faults with a dextral strike–slip component and intra-continental transtensional grabens. Strong uplift rates are documented by thick coarse-grained continental deposits filling these volcano-sedimentary basins and decompression melting processes in orthogneisses and metagraywackes within Aiguilles-Rouges and Mont-Blanc massifs dated at 317–320 Ma (monazite, Bussy and Hernandez, 1997).

The post-collision dominantly granitic magmatic activity consists of very short-lived syn-tectonic episodes of a few Ma, strongly controlled by the transcurrent crustal-scale faults. Early Mg–K-rich magmatism is widely recorded between 345 and 330 Ma from Corsica to the Bohemian massif. High to very high-K plutons were emplaced at 334–333 Ma in Aar massif (Schaltegger and Corfu, 1992) and at 332 Ma in Aiguilles-Rouges massif (Bussy et al., 1998). These magmas probably derived from a subduction-enriched lithospheric mantle source with subsequent crustal contamination, as evidenced by Hf isotopes (Schaltegger and Corfu, 1992) and occurrences of melanocratic stocks or enclaves of vaugneritic to durbachitic composition.

The subsequent magmatic pulse at 310 Ma in Aar massif, thought to derive from a similar source, evolves towards high-K calc-alkaline diorite to granodiorite (Schaltegger and Corfu, 1992). In the Mont-Blanc–Aiguilles-Rouges area, syn-tectonic peraluminous magmas were emplaced along dextral strike–slip faults at 307 Ma. A dominantly crustal source is inferred by Al-rich minerals, restitic xenoliths and high $\delta^{18}O$ values (Brändlein et al., 1994), but mantle contribution is documented by coeval gabbro and mafic microgranular enclaves (Bussy and Hernandez, 1997).

The last magmatic episode is PO and alkali-calcic. It is documented by the 303 Ma Mont-Blanc granite and the 298 Ma Central Aar granite pluton, and by abundant intermediate to acidic volcano-clastic deposits at 303–299 Ma (Schaltegger, 1994). Magmatism in the nearby Gotthard massif is still poorly characterised, with a group of about 300 Ma deformed calc-alkaline diorites–granodiorites–granites and another of 295 to 292 Ma undeformed plutons (Schaltegger, 1994).

The Central Aar Granite (Fig. 4) comprises several discrete bodies of granodiorite, granite, leucogranite and aplite (Table 3), heterogeneously deformed and overprinted by Alpine greenschist facies metamorphism. Biotite is the only mafic mineral and unusual accessories are found in aplitic facies (chernovite, polycrase, thorite). K is high throughout the whole suite. The highly differentiated leucogranitic facies are very low in Ca, Mg and Fe, extremely depleted in Ba, Sr, La and Ti, and relatively enriched in Rb, Y, HREE, Th and U compared to granodiorite. Though ΣREE (200–380 ppm) is not clearly correlated with SiO_2 contents, overall LREE depletion, HREE enrichment and increasing Eu negative anomaly lead to gull wing-shaped patterns and tetrad effects in leucogranite. Fractional crystallisation was the predominant differentiation process. Low initial Sr isotope ratios, positive ε_{Hf} and absence of zircon inherited cores all point to an ultimate mantle source. Evolution of ε_{Hf} values from -8 in ultrapotassic 334 Ma monzonite to $+3.5$ in Central Aar Granite to $+5$ in late lamprophyre

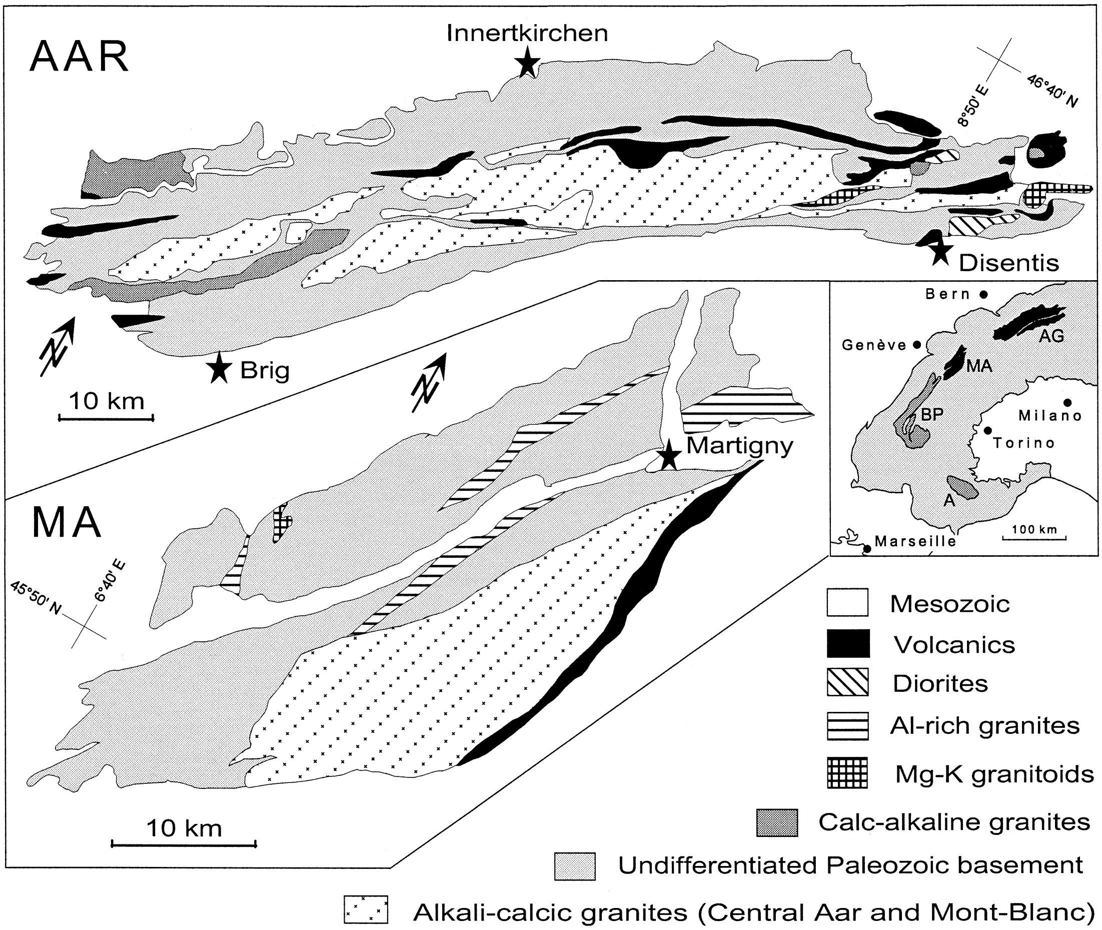

Fig. 4. The Mont Blanc–Aar suite. Sketch map of the Aar Massif (Bonin et al., 1993).

indicates an increasing contribution of the upwelling asthenospheric mantle relative to the subcontinental lithospheric mantle source that produced the 334 Ma rocks (Schaltegger and Corfu, 1992).

The Mont-Blanc granite is strikingly similar to the monzogranitic facies of the Central Aar Granite (Table 3). Biotite composition reflects high Fe/Mg ratio in magmas as opaque minerals are very rare. The Mont-Blanc granite differs mainly from the Central Aar Granite by the presence of numerous mafic microgranular enclaves, calc-alkaline micromonzodioritic stocks and synplutonic dykes, which indicate a mantle source and magma mingling processes. Enriched REE patterns with flat HREE distribution for the most mafic stocks and dykes, as well as inherited 630 Ma zircon cores in the granite, reflect crustal contamination of unknown magnitude. The border zone of the intrusion is occupied by leucogranite quartz–porphyry rich in Rb, Th, U and poor in Sr, Ba.

3.2. The Permo-Triassic Western Mediterranean alkaline province

Present morphological features of the Western Mediterranean area are governed basically by the Alpine orogeny, but all orogenic events having affected this complex zone are recorded through tectonics, magmatism, metamorphism and sedimentation (Von Raumer and Neubauer, 1993, and references therein). The Helvetic realm and the European foreland were affected by the Variscan event which

Table 3
The 300 Ma magmatic suites of Western and Central Alps

		Aar	Mont-Blanc
Rock types		granodiorite Central Aar granite Mittagflue granite Kessiturm aplite	monzodiorite (dykes, stocks) granodiorite (enclaves) granite leucogranite, aplite
Rock-forming mineralogy		quartz + K-feldspar + plagioclase + biotite ± hornblende	quartz + K-feldspar + plagioclase + biotite ± hornblende
Accessory mineralogy		allanite + titanite + zircon + apatite + ilmenite + chernovite + polycrase + thorite + fluorite ± molybdenite	allanite + titanite + zircon + apatite + ilmenite + chernovite + polycrase + thorite + fluorite ± molybdenite
Major element chemistry	SiO_2	63–77 wt.%	55–77 wt.%
	K_2O	3.5–5 wt.%	2.5–6 wt.%
	K_2O/Na_2O	0.7–1.4	0.8–1.7
	ASI	metaluminous to slightly peraluminous alkali-calcic suite	metaluminous to slightly peraluminous alkali-calcic suite
Trace elements (ppm)	Rb	120–280	170–490
	Ba	100–1200	10–800
	Th	20–40	0–50
	Zr	100–300	40–400
	Y	30–100	30–70
REE patterns	La (ppm)	10–50	20–54
	$(La/Yb)_N$	0.3–10.7	1.6–10.6
	Eu/Eu*	0.01–0.34	0.08–0.52
		gull wing shape and tetrad effects in aplitic facies	gull wing shape and tetrad effects in aplitic facies
Isotope ratios	Sri	0.705	0.705
	ε_{Hf}	+1–+3.5	no data
Age of emplacement	298 Ma	303 Ma	

Refs. Schaltegger (1990, 1994), Bussy (1990), Schaltegger and Corfu (1992), Bussy and von Raumer (1993).

ended with 300 Ma short-lived PO magmatic activity. By contrast, the terrane composed of the Austro-Alpine realm, the Southern Alps and the Western Mediterranean coastal areas was affected by successive Palaeozoic events (Bonin, 1997).

After an oceanic stage starting at around 530 Ma, the Caledonian event is marked by 470–430 Ma orogenic calc-alkaline and 425 Ma PO alkaline orthogneisses. The Variscan event is poorly represented by post-collision 340–330 Ma high- to very high-K calc-alkaline massifs generally post-dating crustal anatectic magmatism. The following event is akin to the Alleghanian and displays orogenic magmatic units emplaced during the Upper Carboniferous and the Lower Permian. Calc-alkaline magmatic units constitute huge batholiths, such as the 500 km-long 50 km-wide Corsican–Sardinian Batholith (Orsini, 1980; Zorpi et al., 1989; Cocherie et al., 1994). The older tonalitic units are normal calc-alkaline Cordilleran-type and interpreted as the result of renewed subduction process (Finger and Steyrer, 1990). The younger post-collision high-K calc-alkaline units were unroofed at the beginning of the Permian. During the Lower Permian (300–275 Ma) widespread high to very high-K calc-alkaline and anatectic plutonic–volcanic massifs were emplaced (e.g., Vellutini, 1977; Solé Viñas, 1993; Crevola and Pupin, 1994). These massifs yield trace element and isotopic compositions typical of orogenic magmas derived from a depleted mantle source with a subduction component and contaminated at or near the base of continental crust (Cabanis et al., 1990; Barth et al., 1993; Pinarelli et al., 1993).

The PO to anorogenic Permo-Triassic alkaline province is located mainly within this terrane and distinct magmatic episodes are evidenced by radiometric dates. The Mid-Permian (270 ± 10 Ma) is a critical period marked by emplacement of numerous ring complexes. Like in the Adrar des Iforas no time interval is recorded by radiometric dates between the last high-K calc-alkaline and the first alkaline intrusions at about 280 Ma (Pinarelli et al., 1988). Two magmatic alignments (Bonin et al., 1987), one from Morocco to Costa Brava, Catalonia (Ferrés-Hernández et al., 1997), to Corsica–Sardinia to Esterel (Zheng et al., 1991) to Briançonnais to southern Alps and the second from the French Alps to Vosges-Schwarzwald to the Oslo Rift (Rasmussen et al., 1988), define a Y-shaped fault system associated with large sinistral shear zones (Fig. 5). The magmatic suite (Table 4) is compositionally expanded with scarce basic lava flows and voluminous K-rich red ignimbritic sheets at the volcanic level and gabbro–monzonite–pink syenogranite to subsolvus alkali feldspar granite at the subvolcanic level, suggesting water-rich and oxidising conditions (Bonin, 1990). Initial Sr isotope ratios range from 0.703 up to 0.737 and ε_{Nd} from +0.5 down to −5.8 in the Western Mediterranean province, more primitive values (ε_{Nd} up to +4.6) are found in the Oslo Rift (Trønnes and Brandon, 1992). The extreme values characterise highly evolved Sn–W–Mo mineralised peraluminous granites and match closely those of country rocks at the time of emplacement. In the 275

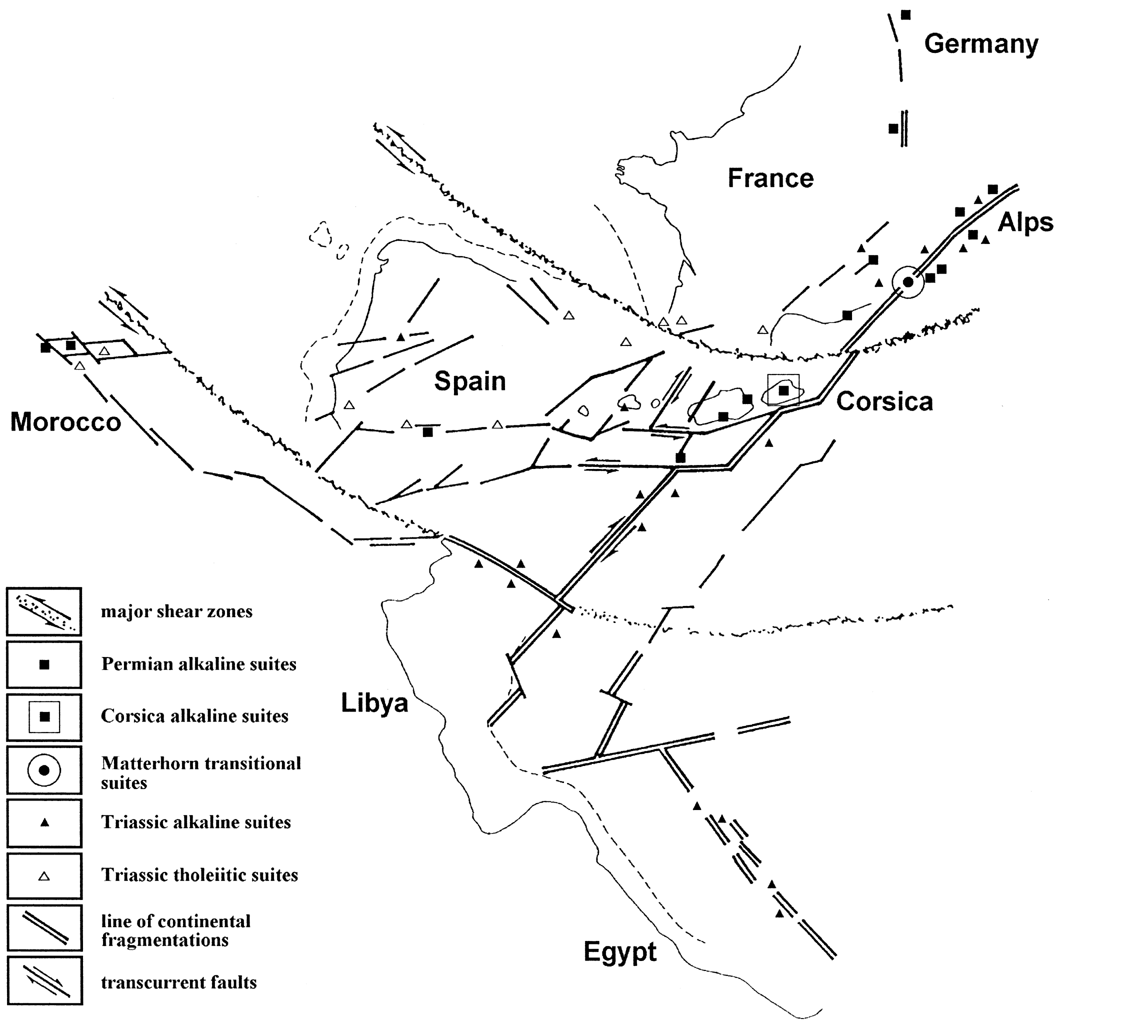

Fig. 5. The Permo-Triassic Western Mediterranean area (Bonin et al., 1987).

Table 4
The Permo-Triassic Western Mediterranean province

Rock types		gabbro and diorite (stocks, enclaves)
		monzonite, syenite
		hypersolvus alkali feldspar granite
		subsolvus syenogranite and alkali feldspar granite
Rock-forming mineralogy		alkali feldspar + quartz ± plagioclase
* Early phases		fayalite + hedenbergite–aegirine augite + hastingsite–hornblende
* Late phases		peraluminous: annite + zinnwaldite–trilithionite + celadonitic muscovite + chlorite
		peralkaline: barroisite–winchite–richterite–arfvedsonite series + grünerite ± riebeckite + aegirine + montdorite
Accessory mineralogy		zircon + allanite + chevkinite + ilmenite + magnetite + apatite + fluorite ± topaz (inclusions within alkali feldspar)
* Mineralised granites		topaz + cassiterite + molybdenite + wolframite + sphalerite + galena + pyrite + pyrrhotite + chalcopyrite
* Peralkaline granites		aenigmatite + elpidite + pyrochlore + thorite + fergusonite ± xenotime ± mimetite
Major element chemistry	SiO_2	60–79 wt.%
	CaO	0.1–2.3 wt.%
	ASI	metaluminous, mildly peraluminous and highly peralkaline alkaline suite
Trace elements (ppm)	Rb	70–550
	Ba	4–1500
	Th	10–87
	Zr	80–2500
	Y	35–240
REE patterns	La (ppm)	4–70
	$(La/Yb)_N$	0.4–3.8
	$Eu/Eu*$	0.01–0.96
		gull wing shape no or slight tetrad effects
Isotope ratios	Sri	0.703–0.737
	ε_{Nd}	+0.5 to −5.8
Age of emplacement		270 ± 10 and 245 ± 10 Ma

Refs. Bonin (1986, 1988), Stille and Buletti (1987), Whalen et al. (1987), Pinarelli et al. (1988), Bonin et al. (1993), Egeberg et al. (1993), Poitrasson et al. (1994, 1995).

Ma gabbro–monzonite–granite Tana-Peloso complex, Corsica (Platevoet, 1990), Sr isotope homogenisation occurred with considerable variations of Nd values and lack of correlation between trace element abundances and isotope ratios precludes simple mixing processes by crustal contamination of mantle-derived magmas (Poitrasson et al., 1994). If the specialised granites are not taken into account, the Sr–Nd–Pb isotope systematics indicate primary magmas having characteristics similar to those of the Ivrea mafic complex (Sinigoi et al., 1994), insignificant to minor contribution of old upper crustal units, varying contribution of lower crust (Pinarelli et al., 1993) and possible involvement of EM1 component in the case of Oslo Rift (Trønnes and Brandon, 1992).

After a quiescent period lasting until the Permian–Triassic boundary (245 ± 10 Ma) larger caldera-related alkaline ring complexes were emplaced in an incipient rifting regime within Corsica, Esterel, Costa Brava of Catalonia, and the Oslo Rift. The magmatic suite is made up of caldera volcanoes filled with basalt lava flows and ignimbritic trachyte–rhyolite and subvolcanic ring complexes containing basic to intermediate rocks and alkali feldspar granites. The aluminous trend comprises metaluminous to peraluminous (more than 1 wt.% CIPW normative corundum) granites and the peralkaline one metaluminous to peralkaline (more than 1 wt.% CIPW normative aegirine and possibly sodium disilicate) granites (Bonin, 1986). Alkali feldspar mineralogy displays hypersolvus, transsolvus and subsolvus assemblages, with subsolvus rock types emplaced after hypersolvus ones (Martin and Bonin, 1976). The paragenesis is complemented by Fe-rich mafic minerals and uncommon Ti (aenigmatite), Pb (mimetite), Zr (elpidite), U, Th, Nb, Ta (pyrochlore), Y (fergusonite), REE-bearing (chevkinite) accessory minerals. Trace element compositions of dolerite dykes indicate derivation from an OIB-type source (Cabanis et al., 1990). Granites yield high, yet variable, LILE and HFSE contents related to [amphibole + plagioclase + alkali feldspar + accessory minerals] fractionation and volatile transfer through F-rich complexing fluids (Egeberg et al., 1993). Peralkaline granites yield lower Sr and higher Nd values than subsolvus biotite granites (Poitrasson et al., 1995).

Last, the Triassic (245–200 Ma) is marked by the onset of Tethys oceanic basin spreading with the development of a large rift system and emplacement of volcanic–plutonic complexes related to strike–slip fault zones. Anorogenic suites are illustrated by the 237–232 Ma Monzoni-Predazzo monzonite–granite alkaline complex, Southern Alps, the 245 Ma Matterhorn–Mont Collon–Dents de Bertol gabbro–granite transitional association, Austro-Alpine realm, and the tholeiitic ophites of Pyrénées. A 200 Ma thermal anomaly has reset most mineral and some whole-rock isotopic dates (D'Amico and Del Moro, 1988), substantiating the link between the last episode of the Western Mediterranean province and the first phase of Tethys ocean evolution (Bonin, 1997).

The Mid-Permian episode is PO, namely post-Alleghanian, and resembles post-collision alkaline suites, such as the post-Pan-African Adrar des Iforas alkaline province, Mali, and the post-Brasiliano Saibro intrusive suite, southern Brazil. The Late Permian to Triassic episode is not post-Alleghanian, but early anorogenic (EA), and resembles true anorogenic alkaline suites, such as the Niger–Nigeria Younger Granite province, west Africa, and the White Mountain Magma Series, New England. It heralds the Mesozoic evolution of the Western Mediterranean area and can be considered as eo-Alpine as well.

4. Characteristics of PO suites

The five examples of PO magmatic suites described above come from world-wide orogenic belts formed at the end of the Precambrian and the Palaeozoic. Actually, PO magmatic suites are common to all orogens known in the world. Other examples taken from older, e.g., Palaeoproterozoic and even Archaean, or younger, e.g., Alpine, could have been used as well. They have in common the fact that they post-date the cessation of main collision deformation and the very late stages of post-collision processes.

4.1. Common features of PO and anorogenic magmatic suites

PO magmatic suites differ from the preceding orogenic suites in that they have higher magmatic temperatures, more primitive isotopic signatures and bimodal rock type distribution. They share characteristics in terms of geological settings, petrological, mineralogical and chemical features in common with within-plate anorogenic suites found in continental or oceanic environments.

(i) Due to rapid decrease of erosion rates after post-collision episodes, the PO suites are observed mainly, not always, as subvolcanic ring complexes and caldera volcanoes, associated with hypabyssal dyke swarms and 1000 km^2-scale volcanic plateaux. They form clusters of 5 to 20 km-wide complexes, aligned along terrane boundary-related thrust and shear zones in transtensional to, more rarely, tensional regimes at a lithospheric scale.

(ii) Basic rocks are scarce. Very rare intermediate rocks evidence Daly gap. Syenogranite and alkali feldspar granite predominate in the magmatic suites. When they are present the anhydrous Fe-bearing to Fe-rich mafic mineral species, such as olivine and calcic clinopyroxene, crystallise near the liquidus. The hydrous calcic amphibole and mica are always later, sometimes near the solidus. Sodic and/or Li-bearing species, such as amphibole, clinopyroxene and mica, precipitate very late and usually below the solidus.

(iii) The highly complex accessory paragenesis is composed of Ti, Zr, U, Th, Nb, Ta, Y and REE-bearing silicates, phosphates, oxides, sulphides, fluorides, and less frequently carbonates and sulphates. Refractory and easily leached mineral species coexist and substantiate the two-fold role played by accessory minerals, either as euhedral crystals in fractionating assemblages at the magmatic stage or as anhedral crystals produced during the hydrothermal stages. According to the Pupin (1980) petrological grid, zircon crystals have *A* indices higher than 600 compared to a maximum value of 700, determined by predominant {101} pyramid, and a spectrum of *T* indices from 800 to 100, marked by decreasing development of {100} prism relative to {110} prism. High *A* indices indicate alkali-rich magmas, while *T* indices are related to crystallisation temperatures and water contents. High and constant growth rates of {010}, relative to pyramidal forms, and symmetric growth of {011} are promoted by high cooling rates (Vavra, 1994). Xenocrystic cores are rare.

(iv) Major and trace element whole-rock chemistries are typical of A-type granites and within-plate granites. In the Whalen et al. (1987) and Eby (1990) compilations, PO suites, namely Malani suite of northern India, A-type granites of Bega Batholith of south-eastern Australia, Topsails, Seal Island and St. Lawrence suites of Newfoundland, the Arabian Peninsula and Corsica, are clearly identified. Eby (1992) uses the critical Y/Nb ratio of 1.2 as the most reliable discriminating factor for a two-fold classification, (i) the intraplate continental rift-related A_1 group has element ratios similar to oceanic-island basalts, (ii) element ratios of the PO A_2 group vary from continental crust to island-arc basalts.

4.2. Petrological and chemical discrimination of PO suites

Two types of suites are distinguished on the basis of petrographical and geochemical data. The first one is made up of the monzonite–*monzogranite*–syenogranite–alkali feldspar granite association. Plagioclase is present throughout the evolutionary trend and albite forms a discrete phase in the most evolved alkali feldspar granite which is, therefore, subsolvus. SiO_2 contents range between 51 and 56 wt.% for molar $(Na_2O + K_2O) = CaO$, defining the suite as *alkali-calcic* (Peacock, 1931). The monzonite–*syenite*–syenogranite–alkali feldspar granite association resembles closely the anorogenic alkaline suites and, at similar SiO_2 contents, whole-rock chemistry is far less calcic. The suite is *alkalic* (Peacock, 1931), i.e., SiO_2 content is less than 51 wt.% for molar $(Na_2O + K_2O) = CaO$. Feldspar mineralogy is either subsolvus with two discrete phases, alkali feldspar and An_{15} oligoclase to pure albite, or hypersolvus with one mesoperthitic alkali feldspar, or transsolvus, a combination of the two former parageneses (Martin and Bonin, 1976).

Liégeois et al. (1998) observe two behaviours of incompatible elements. The LILE (Rb, U, Th and Ta) group is more enriched relatively to the HFSE (Zr, Y and REE) group in high- to very high-K calc-alkaline suites than in alkaline suites. They suggest a sliding normalisation scheme based on the compositionally expanded suite of Telabit-Yenchichi dyke swarms which were emplaced during the onset of late tectonic magmatism in Adrar des Iforas, Mali. The sliding normalisation is done relatively to the calculated sample from the reference series which has the same SiO_2 content than the studied sample (Liégeois et al., 1998). The following parameters will be used in Fig. 6: SNX is the average of Zr, Y, Ce, Sm and Yb normalised ratios, SNY is the average of Rb, Th, U and Ta normalised ratios. Both alkali-calcic and alkaline suites display trends evolving grossly toward increasing SNX and SNY values (Fig. 6, inset).

The alkali-calcic suites (Hoggar, Algeria, and Mont Blanc–Aar–Combeynot, Alps) share a common evolutionary trend (Fig. 6A,B). Granodiorites to syenogranites show weak variations and plot within an area centred at SNX = 1.1 and SNY = 1.7, indicating they evolved approximately along the same path as the reference. Evolved syenogranites and alaskites yield *positive* linear variations ($\Delta SNY/\Delta SNX \approx 1.0$) from the granodiorite–syenogranite values to the extreme values of SNX ≈ 3.0–4.0 and SNY ≈ 3.0–3.2 of the highly differentiated leucocratic facies. LILE and HFSE behave more incompatibly than in the reference.

The alkaline suites (Hoggar, Algeria, Saibro, southern Brazil, and the Western Mediterranean) show more contrasting behaviours (Fig. 6A and C). The peralkaline trend shows a *positive* non-linear correlation with a downward concavity ($\Delta SNY/\Delta SNX$ decreasing from 2.0 to 0.5) from hypersolvus granites plotting at about SNX = 2.5 and SNY = 0.8 to albite granites reaching extreme values of SNX ≈ 7.0 and SNY ≈ 3.2. As usual in peralkaline rocks (Whalen et al., 1987; Eby, 1990) LILE and HFSE are highly incompatible. By contrast the aluminous

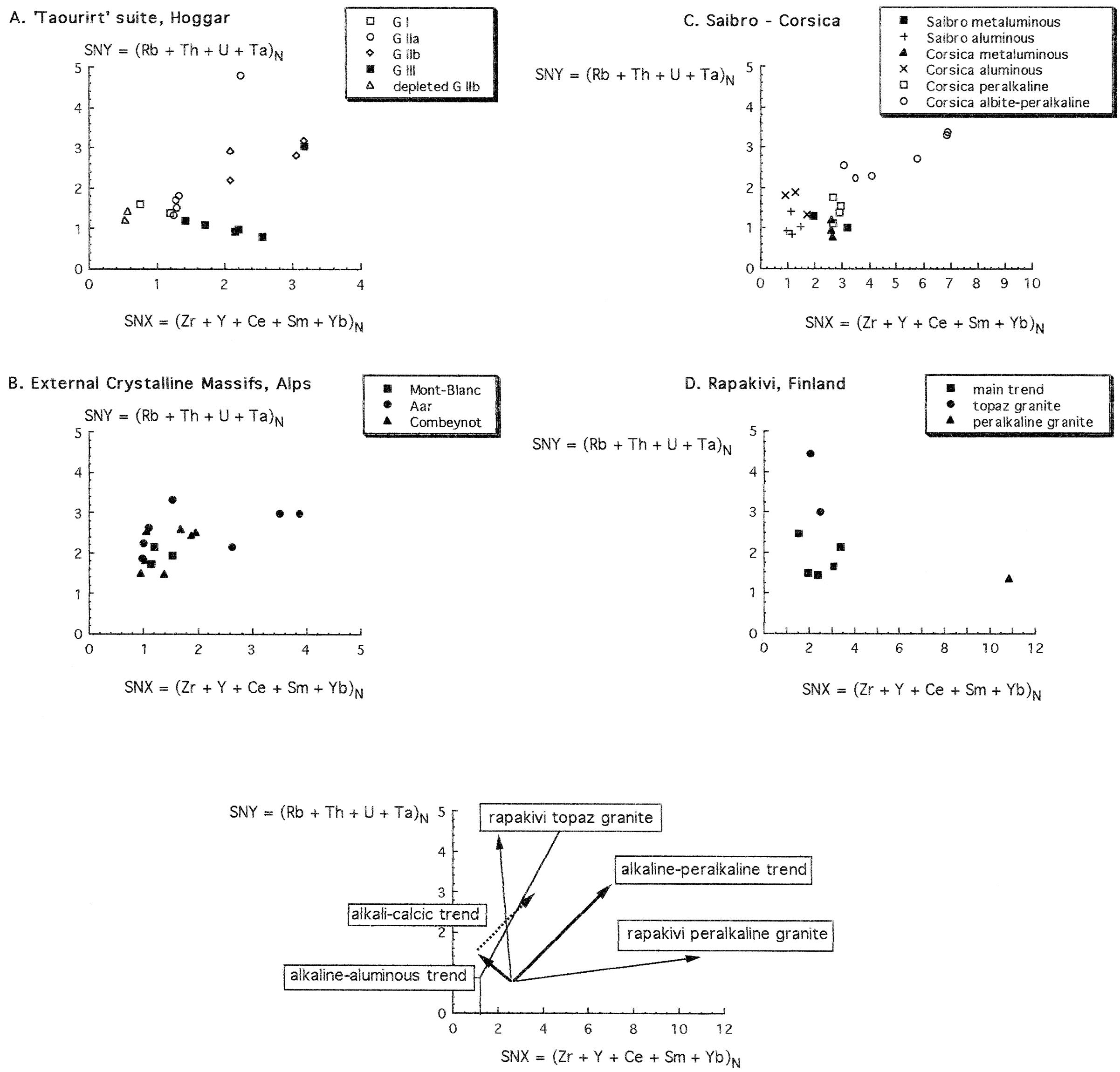

Fig. 6. Normalised (SNX, SNY) plots (Liégeois et al., 1998) of PO suites. (A) 'Taourirt' alkali-calcic suite of Hoggar, Algeria (Zaimen, 1994; Azzouni-Sekkal and Bonin, 1998; unpublished data). (B) Mont Blanc–Aar–Combeynot, External Crystalline Massifs, French and Swiss Alps, alkali-calcic suites (Costarella, 1987; Bussy, 1990; Schaltegger, 1990). (C) Corsica, Western Mediterranean (Whalen et al., 1987; Bonin, 1988), and Saibro, southern Brazil (Nardi and Bonin, 1991; Frantz and Nardi, 1992), alkaline suites. (D) The anorogenic rapakivi alkali-calcic suite, Finland (Rämö, 1991; Rämö and Haapala, 1995). Inset: major trends within PO magmatic suites. Boundaries of fields for syn- and post-collision suites (Liégeois et al., 1998) are shown for comparison.

trend is characterised by *decreasing* SNX values and a weakly *negative* correlation ($\Delta SNY/\Delta SNX \approx 0.0$ to -0.6) from metaluminous granites at $SNX = 2.0$ and $SNY = 1.2$ to peraluminous transsolvus to subsolvus granites plotting at $SNX \approx 1.0$ and $SNY \approx 1.0$–1.8, identical to the alkali-calcic granodiorite–syenogranite values. LILE still continue to be slightly more incompatible than in the Telabit-Yenchichi reference, but HFSE are compatible due to Zr, Y and REE-bearing accessory minerals precipitation.

The anorogenic rapakivi suite is examined for comparison (Fig. 6D). This alkali-calcic suite is composed in Finland of syenite, various types of granite (tirilite, wyborgite, pyterlite), granite–porphyry and low-*P* topaz granite (Rämö, 1991). Peralkaline rocks are abundant in other areas (Rämö and Haapala, 1995). Whole-rock compositions are metaluminous, peraluminous and peralkaline. Protracted behaviours are illustrated by metaluminous granitoids plotting in the same area as PO alkaline granites and extremely high values for peralkaline granite (SNX = 11.0, SNY = 1.4) and topaz granite (SNX = 2.0, SNY = 4.5).

4.3. *Amphibole–biotite antagonism and H_2F_2 vs. H_2O behaviours*

Alkali-calcic and alkaline mixed mafic–felsic complexes provide evidence for derivation of granitic liquids from mafic *intermediate* magmas by crystal fractionation. Granites are governed by crystallisation of hydrous (amphibole, biotite, accessory minerals) and anhydrous (plagioclase, alkali feldspar, Fe–Ti oxides, accessory minerals) phases. The two types of suites differ in that (i) the major hydrous phase to precipitate is biotite in the alkali-calcic suite and amphibole in the alkaline one, and (ii) plagioclase is more abundant in the alkali-calcic suite than in the alkaline one.

Amphibole contains 2 (OH) anions per formula unit. For the same number of 24 oxygen atoms, biotite is twice more hydrous with 4 (OH) a.p.f.u., suggesting that biotite-controlled alkali-calcic residual liquids evolve under higher water fugacities than amphibole-controlled alkaline ones. In the hydroxyl site, (OH) can be replaced by F and/or Cl. In alkali-calcic suites as well as in aluminous subsolvus granites of alkaline suites, fluorite is a frequent accessory mineral. Mg-bearing biotite contains F in relatively low abundance, while late Fe-rich sodic amphiboles in peralkaline granites are F-rich (Bonin, 1988). As F is strongly correlated with Mg due to the Fe–F avoidance effect (Icenhower and London, 1997), the dissolved fluids related to biotite crystallisation in aluminous granites would be less F-rich than those necessitated by sodic amphibole in peralkaline granites. It is suggested that alkaline suites evolve at low pressures under the influence of F-rich fluids while alkali-calcic ones evolve at slightly higher but still shallow pressures with F-bearing more aqueous fluids. F-rich brines carrying large amounts (up to 34 wt.%) of dissolved solids are well known in present geothermal systems in identical geodynamic settings, e.g., Salton Sea, CA (Elders, 1989).

5. The sources problem

In PO alkali-calcic and alkaline suites, mafic and intermediate rocks can differ from granitoids in terms of their Sr–Nd–Pb isotope systematics. This is usually interpreted in terms of mixtures of depleted mantle with low Sr isotope ratios and positive ε_{Nd} and old crust with high Sr isotope ratios and negative ε_{Nd}. Quantitative modelling of the respective roles played by mantle and crustal sources needs to be constrained by known end-member compositions. In post-collision as well as in PO magmatic suites almost no mafic rocks display the expected low Sr isotope ratio and highly positive ε_{Nd} compositions (Stille and Buletti, 1987; Rottura et al., 1997), suggesting that either mafic magmas are heavily contaminated by crust, or the mantle sources have more radiogenic compositions. Crustal contamination can affect mafic intermediate and granitic magmas as well. DePaolo et al. (1992) conclude that crustal contamination plays a prominent role in mafic intermediate magmas because they have enough thermal energy and display chemical gradients high enough to assimilate crustal rocks. Isenthalpic AFC models show that during early stages felsic crust can be assimilated at a rate of up to 20% of the initial basaltic magma mass with only 3–7% crystallisation, resulting in large shifts in isotopic and trace element contents with little major element variations (Reiners et al., 1995).

5.1. *Crustal signatures*

In most provinces a close correlation exists between isotope characteristics and granite types. Isotopic variability does not lead straightforward interpretations and the same isotopic data can be used as evidence for various models, each apparently equally valid. We examine briefly two models, (i) the entirely crustal origin model and (ii) the mantle-derived crustal-contaminated evolving magma model.

(i) The entirely crustal origin model is based on the assumption that, if it is safe to consider mafic magmas as mantle-derived, coeval acidic magmas are crustal and not cogenetic. In this scheme, Nd isotopic variability can be used as evidence for lower crustal signatures (Poitrasson et al., 1994). The major difficulty raised by the entirely crustal origin model is the ability of thin continental crust to produce monzonitic liquids at around 1000°C (Thompson, personal communication, 1990; for a review of melting evidence, see Bonin, 1996).

Baker (1989) and Lesher (1994) show that elements and isotopes do not move at the same velocity and that kinetic disequilibria during mixing processes result in fast and complete Sr isotope equilibration and variable ε_{Nd} levels. Kinetic disequilibria are expected within short-lived magmatic episodes. Another potentially active factor is REE mobility in F-rich complexing fluids (Bau, 1996, and references therein) which can be recognised not by present whole-rock F-contents but by F-rich minerals, e.g., topaz and fluorite, as late minerals or veins. F-rich fluid metasomatism associated with alkaline granites has been documented (e.g., Abdel-Rahman and Martin, 1990).

(ii) The mantle-derived crustal-contaminated evolving magma model is popular since its first mathematical formulation by DePaolo (1981). Poitrasson et al. (1995) suggest two distinct sources, (1) a primitive mantle source with Sr and Nd values close to Bulk Earth for peralkaline granites and (2) lower crustal reservoirs for subsolvus biotite granites while hypersolvus biotite granites would come from mantle magmas that have interacted with lower crust.

Bonin (1986, 1988) concludes that all granite types, the relatively primitive metaluminous as well as the more evolved peraluminous and peralkaline granites, are genetically related through two evolutionary trends. In low-Ca rocks, slight variations of the $(Na+K)/Al$ agpaitic index result easily in a shift from metaluminous to peraluminous and peralkaline compositions. Water favours amphibole stability at low pressures and controls indirectly alumina saturation of late stage liquids. Predominant amphibole, an Al-poor mineral, fractionation leads to peraluminous (CIPW normative corundum, modal biotite and other Al-rich minerals) end products, while predominant feldspar fractionation promotes peralkaline (CIPW normative aegirine, modal sodic mafic and accessory minerals) end products.

Water-undersaturated magmas generated by a primitive mantle source interact with crustal materials. As chemical diffusion at the walls is too sluggish a process to be significant, contamination occurs mainly through discrete vapour phases. Water comes mainly from crust and F from mantle. If little or no aqueous fluids are available, F-rich peralkaline granite magmas suffer little contamination and F-rich fluids are extracted late during emplacement and cooling (Abdel-Rahman and Martin, 1990; Egeberg et al., 1993). In the case of early water saturation peraluminous granite magmas are modified by water percolating within convective geothermal cells (Martin and Bonin, 1976). In this scheme, major and trace element and Sr–Nd–Pb isotope compositions of PO granites are acquired at various periods of magma history and PO granites cannot, therefore, provide clean images of their sources.

5.2. Shifts in the cooling lithosphere

Because they can move upwards at velocities up to more than 1 m s^{-1}, the minimum speed necessary for entrainment of xenoliths (Emerman and Marrett, 1990), primitive Cr–Ni-rich high-Mg mafic dykes constitute more reliable probes of mantle chemistry. Late Palaeozoic high to very high-K calc-alkaline lamprophyres yield high LILE abundances and variable radiogenic isotope ratios, suggesting that mantle sources were affected by different degrees of K-metasomatism through fluids related to the ending stages of subduction. In the Southern Alps appinitic dykes have variable Sr and Pb isotope ratios suggesting two mantle radiogenic sources and contamination by lower crust formations (Pinarelli et al., 1988, 1993). In the Bohemian Massif (Holub et al., 1997), Sr isotope ratios and ε_{Nd} shift, respectively, from 0.705/+0.1 in the 349 Ma medium-K calc-alkaline gabbro to extreme values of 0.713/-8.6 in the 343 Ma primitive Cr–Ni-rich very high-K durbachite, illustrating large mantle variability (Janousek et al., 1995). Then, isotope compositions of very high-K calc-alkaline granitoids do not reflect high degrees of crustal assimilation during magma ascent through the continental crust, but more likely the amount of crustal products afforded to the metasomatised mantle source itself.

In the Late Palaeozoic PO magmatic suites, dolerite dykes and lava flows indicate derivation from an OIB source. The *least contaminated* mafic and intermediate rocks and peralkaline granites suggest a source close to Bulk Earth, substantiating a very fast shift from depleted mantle sources flushed by subducted crustal materials to a more primitive LILE and HFSE-rich source. A similar shift is documented in the late to post-Pan-African Adrar des Iforas (Liégeois, 1988; Liégeois et al., 1998).

Localisation of the different mantle source regions is a matter of debate (see Arndt et al., 1993; Hawkesworth and Gallagher, 1993; Smith, 1993; Anderson, 1994). The depleted source region is ascribed to convecting MORB asthenosphere, but the variously enriched source regions have been suggested to lie within subcontinental lithosphere as well as deeply rooted plume heads. The concept of enriched source itself needs further refinement. McKenzie and O'Nions (1995) define two types of enriched source regions, (i) in western Turkey and the Aegean Sea they must have been previously *depleted* and later *enriched* by addition of metasomatic liquids and fluids and (ii) non-orogenic oceanic islands do not require their source regions to have been depleted before being enriched. The thermo-mechanical model derived from this observation (McKenzie and O'Nions, 1995, Fig. 17, p. 155) may help to explain the succession of the last stages of an orogenic event (Black and Liégeois, 1993, Fig. 4, p. 92). The depleted/enriched (in the sense of McKenzie and O'Nions) source regions are less dense than the MORB source and constitute the lithospheric mechanical boundary layer. The undepleted/enriched heavier source regions correspond to lower parts of the lithospheric thermal boundary layer and can be easily entrained into thermal convection and removed by sinking thermal plumes causing lithosphere delamination. Later, they can be advected upwards by plumes beneath continents and/or oceans. Magmas can be generated by wet (dehydration) melting below the dry solidus and produced either within the mechanical boundary layer by heat conducted from plumes, or within the ascending plume metasomatised regions.

5.3. Implications for post-collision magmatic suites

This thermo-mechanical model can explain why, in some orogenic areas, the latest high to very high-K calc-alkaline post-collision suites with an enriched/depleted signature were emplaced at nearly the same time as the earliest PO suites with an enriched but *not* depleted signature (e.g., the 560–540 Ma period in the Adrar des Iforas, Mali, and the 270 $\pm$ 10 Ma period in the Western Mediterranean). In this case replacement of 'old' lithospheric mantle by a new source coming from below is a very fast process. By contrast in other orogenic areas, such as the Upper Precambrian Hoggar and Sul-rio-grandense shields and the Variscan European foreland of the Alpine belt, high to very high-K calc-alkaline post-collision suites were generated by melting of phlogopite-bearing metasomatised parts of mechanical boundary layer well before (up to 100–200 Ma and 40 Ma, respectively) any intervention by ascending thermal plumes and the generation of PO suites. The evolution towards very high-K compositions could be related to progressive fading of thermal anomalies inducing lower degrees of wet melting of the cooling metasomatised parts of the mechanical boundary layer.

In all cases PO suites were synchronous throughout the orogen, whether they were immediately preceded by high- to very high-K calc-alkaline suites, or not. This observation supports the idea that PO magmatic episodes could be more closely related to subsequent break up of Pangaea than to waning orogenic episodes developing within the cooling subcontinental lithosphere. It also explains why they make way so rapidly to anorogenic magmatic episodes (Bonin, 1990). Later on, reactivating of lithospheric fault zones and initiation of continental rifts result in lithospheric thinning. Related magmatic suites tend to be sodic and derived from convecting mantle sources at the rift axis and potassic and derived from subcontinental lithospheric mantle at the margins of the thinned zone (Thompson and Gibson, 1994).

6. Summary and conclusions: the very end of the orogenic Wilson cycle

The orogenic Wilson cycle ends with a dominantly ensialic episode consisting of accretion of continental blocks or terranes. In the internal parts of the orogenic belts, numerous magmatic episodes correspond to various sources and differentiation processes within geodynamic settings evolving from subduction-related to anorogenic.

The post-collision event starts with processes still influenced by crustal materials subducted below the orogenic subcontinental lithospheric mantle. The dominantly calc-alkaline suites document a shift from normal to high to very high-K associations. Differentiation is governed by nearly water-saturated environments, inducing crystallisation of Mg-rich amphibole and biotite as early as within primitive Cr–Ni-rich mafic magmas with lamprophyric affinities (vaugnerite–durbachite association), accompanied by magma mingling/mixing processes. Source regions are composed of depleted and later enriched orogenic subcontinental lithospheric mantle, affected by dehydration melting under a cooling regime and generating decreasing volumes of more and more K- and LILE-rich magmas. In the vicinity of intra-crustal magma chambers, anatexis may occur by incongruent melting of hydrous minerals, such as biotite, generating peraluminous granitoids bearing mafic micro-granular enclaves.

The end of the post-collision event is marked by the onset of emplacement of PO suites. They are exposed as volcanic plateaux, dyke swarms, caldera volcanoes and subvolcanic ring complexes, aligned along large transcurrent fault zones created during collision and reactivated later. Bimodal suites contain scarce basic rocks, almost no intermediate rocks and predominant granitoids. Two types of suites are defined, (i) the alkali-calcic monzonite–monzogranite–syenogranite–alkali feldspar granite association characterised by [biotite + plagioclase] fractionation and moderate [LILE + HFSE] enrichments, with the exception of late-stage alkali feldspar granites and (ii) the alkaline monzonite–syenite–alkali feldspar granite association with two evolutionary trends characterised by [amphibole + alkali feldspar] fractionation, the peralkaline trend yielding sodic mafic mineralogy and higher enrichments in HFSE than in LILE and the aluminous biotite-bearing trend marked by HFSE depletion relatively to LILE due to accessory mineral precipitation. Alkali-calcic and alkaline evolutionary trends differ essentially by the amounts of water present within intra-crustal magma chambers. In presence of abundant water biotite is the chief mafic mineral in plagioclase-rich cumulus assemblages and the resulting trend is alkali-calcic. In water-poor environments, amphibole precipitates and the resulting trend is silica-saturated to oversaturated alkaline.

PO suites originate in identical enriched and not depleted mantle source, whatever the precipitating assemblages within magma chambers. The more primitive LILE and HFSE-rich source rapidly replaces the older orogenic subcontinental lithospheric mantle source during lithosphere delamination and becomes progressively the new thermal boundary layer part of the subcontinental lithosphere mantle. During the ascent, storage and differentiation at different levels of the continental crust, mantle-derived magmas experience crustal assimilation and contamination. Present rock compositions are composed of a mixture of the major mantle contribution and of various crustal components. No induced anatexis of wall rocks has been observed, suggesting that crustal contamination could occur predominantly through F-rich aqueous fluids circulating within convective geothermal cells created around magma chambers.

PO suites correspond to the last magmatic episodes in an orogenic belt which becomes progressively a craton by cooling and thickening of lithosphere. In favourable areas these magmatic suites herald initiation of Pangaea break up and pre-date a new orogenic Wilson cycle.

Acknowledgements

We gratefully acknowledge supports by the French Ministry of Foreign Affairs through Accord-Programme #94 MDU 282, the Brazilian CNPq and the Swiss NFS grants #8220-028439 and 21-45650. We are indebted to R. Black, D. Boztug, J.P. Liégeois, D. Marquer, L.V.S. Nardi, A. Rottura, U. Schaltegger, A.B. Thompson, D. Visonà and J. von Raumer for exchanges of ideas on this subject. G.N. Eby and F. Poitrasson by their useful reviews helped us to

clarify the ideas presented here. Finally, we would like to express our admiration of the pre-eminent role played by R. Black in continued research on geodynamic settings in the Pan-African domains.

References

Abdel-Rahman, A.M., Martin, R.F., 1990. The Mount Gharib A-type granite, Nubian Shield: petrogenesis and role of metasomatism at the source. Contrib. Mineral. Petrol. 104, 173–183.

de Almeida, F.F.M., Hasui, Y., Brito Neves, B.B., Fuck, R.A., 1981. Brazilian structural provinces: an introduction. Earth Sci. Reviews 17, 1–29.

Anderson, D.L., 1994. The sublithospheric mantle as the source of continental flood basalts; the case against the continental lithosphere and plume head reservoirs. Earth Planet. Sci. Lett. 123, 269–280.

Arndt, N.T., Czamanske, G.K., Wooden, J.L., Fedorenko, V.A., 1993. Mantle and crustal contributions to continental flood volcanism. Tectonophysics 223, 39–52.

Azzouni-Sekkal, A., Boissonnas, J., 1993. Une province magmatique de transition du calco-alcalin à l'alcalin: les granitoïdes pan-africains à structure annulaire de la chaîne pharusienne du Hoggar (Algérie). Bull. Soc. Géol. Fr. 164, 597–608.

Azzouni-Sekkal, A., Bonin, B., 1998. Les minéraux accessoires des granitoïdes de la suite 'taourirt', Hoggar (Algérie): conséquences pétrogénétiques. J. Afr. Earth Sci. 26, 65–87.

Baker, D.R., 1989. Tracer versus trace element diffusion: diffusional decoupling of Sr concentration from Sr isotope composition. Geochim. Cosmochim. Acta 53, 3015–3023.

Barbarin, B., 1990. Granitoids: main petrogenetic classifications in relation to origin and tectonic setting. Geol. J. 25, 227–238.

Barth, S., Oberli, F., Meier, M., Blattner, P., Bargossi, G.M., Di Battistini, G., 1993. The evolution of a calc-alkaline basic to silicic magma system: Geochemical and Rb–Sr, Sm–Nd, and $^{18}O/^{16}O$ isotopic evidence from the Late Hercynian Atesina Cima d'Asta volcano-plutonic complex, northern Italy. Geochim. Cosmochim. Acta 57, 4285–4300.

Bau, M., 1996. Controls on the fractionation of isovalent trace elements in magmatic and aqueous systems: evidence from Y/Ho, Zr/Hf, and lanthanide tetrad effect. Contrib. Mineral. Petrol. 123, 323–333.

Bertrand, J.M., Michard, A., Boullier, A.M., Dautel, D., 1986. Structure and U–Pb geochronology of the Central Hoggar (Algeria). A reappraisal of its Pan-African evolution. Tectonics 5, 955–972.

Bitencourt, M. de F., Remus, M.V., Nardi, L.V.S., 1987. Complexos graníticos da região oeste do escudo sul-rio-grandense. 1°Congr. Bras. Geoqu., Excursões, Porto Alegre, 55–90.

Black, R., Liégeois, J.P., 1993. Cratons, mobile belts, alkaline rocks and continental lithospheric mantle: the Pan-African testimony. J. Geol. Soc., London 150, 89–98.

Black, R., Caby, R., Moussine-Pouchkine, A., Bayer, R., Bertrand, J.M.L., Boullier, A.M., Fabre, J., Lesquer, A., 1979. Evidence for late Precambrian plate tectonics in Africa. Nature 278, 223–227.

Black, R., Lameyre, J., Bonin, B., 1985. The structural setting of alkaline complexes. J. Afr. Earth Sci. 3, 5–16.

Black, R., Latouche, L., Liégeois, J.P., Caby, R., Bertrand, J.M., 1994. Pan-African displaced terranes in the Tuareg shield (central Sahara). Geology 22, 641–644.

Bonin, B., 1986. Ring complex granites and anorogenic magmatism. Studies in Geology, North Oxford Academic, Oxford, and Elsevier, Amsterdam, 188 pp.

Bonin, B., 1988. Peralkaline granites in Corsica: some petrological and geochemical constraints. Rend. Soc. Ital. Mineral. Petrol. 43, 281–306.

Bonin, B., 1990. From orogenic to anorogenic settings: evolution of granitoid suites after a major orogenesis. Geol. J., W.S. Pitcher Spec. Issue, Vol. 25, pp. 261–270.

Bonin, B., 1996. A-type granite ring complexes: mantle origin through crustal filters and the anorthosite–rapakivi magmatism connection. In: Demaiffe, D. (Ed.), Petrology and Geochemistry of Magmatic Suites of Rocks in the Continental and Oceanic Crusts. A volume dedicated to Professor J. Michot, ULB-MRAC, Bruxelles, pp. 201–217.

Bonin, B., 1997. Late Variscan magmatic evolution of the Alpine belt: an overview. In: Sinha, A.K., Sassi, F.PP., Papanikolaou, D. (Eds.), Geodynamic Domains in the Alpine–Himalayan Tethys. Oxford and IBH Publishing Pvt., New Delhi and A.A. Balkema, Rotterdam, pp. 295–314.

Bonin, B., Platevoet, B., Vialette, Y., 1987. The geodynamic significance of alkaline magmatism in the Western Mediterranean compared with West Africa. In: Bowden, P., Kinnaird, J. (Eds.), African Geology Reviews. Geol. J., Vol. 22, pp. 361–387.

Bonin, B. (Coordinator), Brändlein, P., Bussy, F., Desmons, J., Eggenberger, U., Finger, F., Graf, K., Marro, Ch., Mercolli, F., Oberhänsli, R., Ploquin, A., von Quadt, A., von Raumer, J., Schaltegger, U., Steyrer, H.P., Visonà, D., Vivier, G., 1993. Late Variscan Magmatic Evolution of the Alpine Basement. In: von Raumer, J.F., Neubauer, F. (Eds.), Pre-Mesozoic Geology in the Alps. Springer-Verlag, Berlin, pp. 171–201.

Brändlein, P.P., Nollau, G., Sharp, Z., von Raumer, J., 1994. Petrography and geochemistry of the Vallorcine granite (Aiguilles-Rouges massif Western Alps). Schweiz. Mineral. Petrogr. Mitt. 74, 227–243.

Bussy, F., 1990. Pétrogenèse des enclaves microgrenues associées aux granitoïdes calco-alcalins: exemple des massifs varisque du Mont-Blanc (Alpes Occidentales) et miocène du Monte Capanne (Île d'Elbe, Italie). PhD Thesis, Université de Lausanne. Mémoires de Géologie (Lausanne) 7, 309 pp.

Bussy, F., Hernandez, J., 1997. Short-lived bimodal magmatism at 307 Ma in the Mont-Blanc/Aiguilles-Rouges area: a combination of decompression melting, basaltic underplating and crustal fracturing. Quaderni Geodinamica Alpina e Quaternaria, Milano 4, 22, Abstract.

Bussy, F., von Raumer, J., 1993. U–Pb dating of Paleozoic events in the Mont-Blanc crystalline massif, Western Alps. EUG 7, Strasbourg, Terra Nova, 5: Abstract Supplement 1, 382.

Bussy, F., Délitroz, D., Fellay, R., Hernandez, J., 1998. The Pormenaz monzonite (Aiguilles-Rouges, western Alps): an additional evidence for a 330 Ma-old magnesio-potassic magmatic suite in the Variscan Alps. Schweiz. Mineral. Petrogr. Mitt. 78, 193–194.

Cabanis, B., Cochemé, J.J., Vellutini, P.J., Joron, J.L., Treuil, M., 1990. Post-collisional Permian volcanism in northwestern Corsica: an assessment based on mineralogy and trace-element geochemistry. J. Volc. Geotherm. Res. 44, 51–67.

Caby, R., 1989. Precambrian terranes of Benin–Nigeria and northeast Brazil and the Late Proterozoic south Atlantic fit. Geol. Soc. Am. Spec. Paper 230, 145–157.

Cahen, L., Snelling, N.J., Delhal, J., Vail, J.R., 1984. The Geochronology and Evolution of Africa. Clarendon Press, Oxford, 512 pp.

Cheilletz, A., Bertrand, J.M., Charoy, B., Moulahoum, O., Bouabsa, L., Farrar, E., Zimmermann, J.L., Dautel, D., Archibald, D.A., Boullier, A.M., 1993. Géochimie et géochronologie Rb–Sr, K–Ar et $^{40}Ar/^{39}Ar$ des complexes granitiques pan-africains de la région de Tamanrasset (Algérie): relations avec les minéralisations Sn–W associées et l'évolution tectonique du Hoggar central. Bull. Soc. Géol. Fr. 163, 733–750.

Cocherie, A., Rossi, P., Fouillac, A.M., Vidal, P.P., 1994. Relative importance of recycled- and mantle-derived material in granitoid genesis: An example from the Variscan batholith of Corsica studied by trace element and Nd–Sr–O isotope systematics. Chem. Geol. 115, 173–211.

Costarella, R., 1987. Le complexe annulaire alcalin de Combeynot (Massifs Cristallins Externes, Alpes françaises), témoin d'un magmatisme en régime distensif. Pétrogéochimie et signification géodynamique. PhD Thesis, Université Scientifique, Technologique et Médicale de Grenoble, Grenoble, 268 pp.

Crevola, G., Pupin, J.P., 1994. Crystalline Provence: structure and Variscan evolution. In: Keppie, J.D. (Ed.), Pre-Mesozoic Geology in France and Related Areas. Springer-Verlag, Berlin, pp. 426–441.

D'Amico, C., Del Moro, A., 1988. Permian and Triassic Rb–Sr dating in the Permian rhyodacitic ignimbrites of Trentino (Southern Alps). Rend. Soc. Ital. Mineral. Petrol. 43, 171–180.

DePaolo, D.J., 1981. Trace element and isotopic effects of combined wallrock assimilation and fractional crystallization. Earth Planet. Sci. Lett. 53, 189–202.

DePaolo, D.J., Perry, F.V., Baldridge, W.S., 1992. Crustal versus mantle sources in granitic magmas: a two-parameter model based on Nd isotopic studies. Trans. R. Soc. Edinb.: Earth Sci. 83, 439–446.

Dewey, J.F., 1988. Lithospheric stress, deformation, and tectonic cycles: the disruption of Pangaea and the closure of Tethys. In: Audley-Charles, M.G., Hallam, A. (Eds.), Gondwana and Tethys. Geol. Soc. Spec. Publ. 37, London, pp. 23–40.

D'Lemos, R.S., Strachan, R.A., Topley, C.G., 1990. The Cadomian orogeny in the North Armorican Massif: a review. In: D'Lemos, R.S., Strachan, R.A., Topley, C.G. (Eds.), The Cadomian Orogeny. Geol. Soc. Spec. Publ. 51, London, pp. 3–12.

Eby, G.N., 1990. The A-type granitoids: a review of their occurrence and chemical characteristics and speculations on their petrogenesis. Lithos 26, 115–134.

Eby, G.N., 1992. Chemical subdivision of the A-type granitoids: petrogenetic and tectonic implications. Geology 20, 641–644.

Egeberg, A.T., Bonin, B., Sørensen, H., 1993. The Bonifatto peralkaline granites (NW Corsica): a possible case of evolution through volatile transfer. Bull. Soc. Géol. Fr. 164, 739–758.

Elders, W.A. (Ed.), 1989. A compendium of reports on the Salton Sea Scientific Drilling Project. Salton Sea Scientific Drilling Project 1985–1986.

Emerman, S.H., Marrett, R., 1990. Why dikes?. Geology 18, 231–233.

Fabre, J., 1988. Les séries Paléozoïques d'Afrique: une approche. J. Afr. Earth Sci. 7, 1–40.

Ferrés-Hernández, M., Enrique-Gisbert, P., Delaloye, M., Singer B.S., 1997. Magmatic and thermal history of the central Catalan Coastal Batholith (NE Spain): new constraints from $^{40}Ar/^{39}Ar$ incremental-heating studies. EUG 9, Strasbourg, Terra Nova, 9: Abstract Supplement 1, 503.

Finger, F., Steyrer, H.P., 1990. I-type granitoids as indicators of a Late Paleozoic convergent ocean–continent margin along the southern flank of the central European Variscan orogen. Geology 18, 1207–1210.

Frantz, J.C., Nardi, L.V.S., 1992. Litoquímica e evolução de granitóides cálcio-alcalinos da região leste do Escudo Sul-riograndense. Pesquisas 19, 13–25.

Hawkesworth, C.J., Gallagher, K., 1993. Mantle hotspots, plumes and regional tectonics as causes of intraplate magmatism. Terra Nova 5, 552–559.

Holub, F.V., Machart, J., Manová, M., 1997. The Central Bohemian plutonic complex: geology, chemical composition and genetic interpretation. Sbor. Geol. Ved, Lozisk. Geol. Mineral. 31, 27–50.

Icenhower, J.P.P., London, D., 1997. Partitioning of fluorine and chlorine between biotite and granitic magma: experimental calibration at 200 MPa H_2O. Contrib. Mineral. Petrol. 127, 17–29.

Janousek, V., Rogers, G., Bowes, D.R., 1995. Sr–Nd isotopic constraints on the petrogenesis of the Central Bohemian Pluton, Czech Republic. Geol. Rundsch. 84, 520–534.

Kennedy, W.Q., 1964. The structural differentiation of Africa in the Pan-African ($\pm$500 m.y.) tectonic episode. Ann. Repp. Res. Inst. Afr. Geol., University of Leeds 8, 48–49.

Lameyre, J., Bonin, B., 1993. Granites in the main plutonic series. In: Didier, J., Barbarin, B., (Eds.), Enclaves and Granite Petrology. Developments in Petrology 13, Elsevier, Amsterdam, pp. 3–17.

Lesher, C.E., 1994. Kinetics of Sr and Nd exchange in silicate liquids: theory, experiments, and application to uphill diffusion, isotopic equilibration, and irreversible mixing of magmas. J. Geophys. Res. 99, 9585–9604.

Liégeois, J.P., 1988. Le batholite composite de l'Adrar des Iforas (Mali). Musée Royal de l'Afrique Centrale, annales—série in-8°—Sciences géologiques—95, Tervuren, 231 pp.

Liégeois, J.P., Black, R., 1987. Alkaline magmatism subsequent to collision in the Pan-African belt of the Adrar des Iforas

(Mali). In: Fitton, J.G., Upton, B.G.J. (Eds.), Alkaline Igneous Rocks. Geol. Soc. Spec. Publ. 30, London, pp. 381–401.

Liégeois, J.P., Bertrand, J.M., Black, R., 1987. The subduction- and collision-related Pan-African composite batholith of the Adrar des Iforas (Mali): a review. In: Bowden, P., Kinnaird, J. (Eds.), African Geology Reviews. Geol. J., Vol. 22, pp. 185–211.

Liégeois, J.P., Navez, J., Hertogen, J., Black, R., 1998. Contrasting origins of post-collisional high-K calc-alkaline-shoshonitic and alkaline–peralkaline granitoids. The use of sliding normalization. Lithos, this volume.

Maniar, P.D., Piccoli, P.P.M., 1989. Tectonic discrimination of granitoids. Geol. Soc. Am. Bull. 101, 635–643.

Martin, R.F., Bonin, B., 1976. Water and magma genesis: the association hypersolvus granite–subsolvus granite. Can. Mineral. 14, 228–237.

McKenzie, R., O'Nions, R.K., 1995. The source regions of ocean island basalts. J. Petrol. 36, 133–159.

Nardi, L.V.S., Bitencourt, M.deF., 1989. Geologia, petrologia e geoquímica do complexo granítico de Caçapava do Sul RS. Rev. Bras. Geoc. 19, 153–169.

Nardi, L.V.S., Bonin, B., 1991. Post-orogenic and non-orogenic alkaline granite associations: the Saibro intrusive suite, southern Brazil—a case study. Chem. Geol. 92, 197–211.

Nardi, L.V.S., Frantz, J.C., 1995. The Cordilhera intrusive suite: late Proterozoic peraluminous granitoids from southern Brazil. J. S. Am. Earth Sci. 8, 55–63.

Nardi, L.V.S., de Lima, E.F., 1985. A associação shoshonítica de Lavras do Sul RS. Rev. Bras. Geoc. 15, 139–146.

Oberli, F., Meier, M., Biino, G.G., 1994. Time constraints on the pre-Variscan magmatic/metamorphic evolution of the Gotthard and Tavetsch units derived from single-zircon U–Pb results. Schweiz. Mineral. Petrogr. Mitt. 74, 483–488.

Orsini, J.B., 1980. Le batholite corso-sarde: anatomie d'un batholite hercynien. Composition, structure, organisation d'ensemble. Sa place dans la chaîne varisque française. DSc Thesis, Université Aix-Marseille III, Marseille, 439 pp.

Paquette, J.L., Ménot, R.P., Peucat, J.J., 1989. REE, Sm–Nd and U–Pb zircon study of eclogites from the Alpine External Massifs (Western Alps): evidence for crustal contamination. Earth Planet. Sci. Lett. 96, 181–198.

Peacock, M.A., 1931. Classification of igneous rocks. J. Geol. 39, 54–67.

Pearce, J.A., Harris, N.B.W., Tindle, A.G., 1984. Trace element discrimination diagrams for the tectonic interpretation of granitic rocks. J. Petrol. 25, 956–983.

Pinarelli, L., Boriani, A., Del Moro, A., 1988. Rb–Sr geochronology of Lower Permian plutonism in Massiccio dei Laghi, Southern Alps (NW Italy). Rend. Soc. Ital. Mineral. Petrol. 43, 411–428.

Pinarelli, L., Boriani, A., Del Moro, A., 1993. The Pb isotopic systematics during crustal contamination of subcrustal magmas: the Hercynian magmatism in the Serie dei Laghi (Southern Alps Italy). Lithos 31, 51–61.

Platevoet, B., 1990. Le plutonisme basique et intermédiaire dans le magmatisme anorogénique de Corse. DSc Thesis, Université de Paris-Sud, Orsay, 526 pp.

Poitrasson, F., Pin, C., Duthou, J.L., Platevoet, B., 1994. Aluminous subsolvus anorogenic granite genesis in the light of Nd isotopic heterogeneity. Chem. Geol. 112, 199–219.

Poitrasson, F., Pin, C., Duthou, J.L., 1995. The relationship between petrology and Nd isotopes as evidence for contrasting anorogenic granite genesis: example of the Corsican province (SE France). J. Petrol. 36, 1251–1274.

Pupin, J.P., 1980. Zircon and granite petrology. Contrib. Mineral. Petrol. 73, 207–220.

Rämö, O.T., 1991. Petrogenesis of the Proterozoic rapakivi granites and related basic rocks of southeastern Fennoscandia: Nd and Pb isotopic and general geochemical constraints. Geol. Surv. Finland Bull. 355, 161.

Rämö, O.T., Haapala, I., 1995. One hundred years of Rapakivi Granite. Mineral. Petrol. 52, 129–185.

Rasmussen, E., Neumann, E.R., Andersen, T., Sundvoll, B., Fjerdingstad, V., Stabel, A., 1988. Petrogenetic processes associated with intermediate and silicic magmatism in the Oslo rift, south-east Norway. Mineral. Mag. 52, 293–307.

Reiners, P.W., Nelson, B.K., Ghiorso, M.S., 1995. Assimilation of felsic crust by basaltic magma: thermal limits and extents of crustal contamination of mantle-derived magmas. Geology 23, 563–566.

Rottura, A., Del Moro, A., Caggianelli, A., Bargossi, G.M., Gasparotto, G., 1997. Petrogenesis of the Monte Croce granitoids in the context of Permian magmatism in the southern Alps Italy. Eur. J. Mineral. 9, 1293–1310.

Schaltegger, U., 1990. The Central Aar Granite: highly differentiated calc-alkaline magmatism in the Aar Massif (Central Alps Switzerland). Eur. J. Mineral. 2, 245–259.

Schaltegger, U., 1994. Unravelling the pre-Mesozoic history of Aar and Gotthard massifs (Central Alps) by isotopic dating—a review. Schweiz. Mineral. Petrogr. Mitt. 74, 41–51.

Schaltegger, U., Corfu, F., 1992. The age and source of late Hercynian magmatism in the central Alps: evidence from precise U–Pb ages and initial Hf isotopes. Contrib. Mineral. Petrol. 111, 329–344.

Sinigoi, S., Quick, J.E., Clemens-Knott, D., Mayer, A., Demarchi, G., Mazzuchelli, M., Negrini, L., Rivalenti, G., 1994. Chemical evolution of a large mafic intrusion in the lower crust, Ivrea Verbano Zone, northern Italy. J. Geophys. Res. 99, 21575–21590.

Smith, A.D., 1993. The continental mantle as a source for hotspot volcanism. Terra Nova 5, 452–460.

Solé Viñas, J., 1993. Le massif granitique du Montnegre (Sud de la Costa Brava, Catalogne). Étude pétrologique, géochimique et géochronologique. PhD Thesis, Université de Genève, Genève, 201 pp.

Stille, P., Buletti, M., 1987. Nd–Sr isotopic characteristics of the Lugano volcanic rocks and constraints on the continental crust formation in the South Alpine domain (N-Italy–Switzerland). Contrib. Mineral. Petrol. 96, 140–150.

Taylor, R.P., 1992. Petrological and geochemical characteristics of the Pleasant Ridge zinnwaldite–topaz granite, southern New Brunswick, and comparisons with other topaz-bearing felsic rocks. Can. Mineral. 30, 895–921.

Thompson, R.N., Gibson, S.A., 1994. Magmatic expression of lithospheric thinning across continental rifts. Tectonophysics 233, 41–68.

Trønnes, R.G., Brandon, A.D., 1992. Mildly peraluminous high-silica granites in a continental rift: the Drammen and Finnemarka batholiths Oslo Rift, Norway. Contrib. Mineral. Petrol. 109, 275–294.

Turner, S., Sandiford, M., Foden, J., 1992. Some geodynamic and compositional constraints on 'postorogenic' magmatism. Geology 20, 931–934.

Vauchez, A., Barruol, G., Tommasi, A., 1997. Why do continents break-up parallel to ancient orogenic belts?. Terra Nova 9, 62–66.

Vavra, G., 1994. Systematics of internal zircon morphology in major Variscan granitoid types. Contrib. Mineral. Petrol. 117, 331–344.

Vellutini, P., 1977. Le magmatisme permien de la Corse du Nord-Ouest. Son extension en Méditerranée occidentale. DSc Thesis, Université Aix-Marseille III, Marseille, 276 pp.

Von Raumer, J.F., Neubauer, F. (Eds.), 1993. Pre-Mesozoic Geology in the Alps. Springer-Verlag, Berlin, 677 pp.

Wenzel, T., Hengst, M., Pilot, J., 1993. The plutonic rocks of the Elbe valley-zone (Germany): evidence for magmatic development from single-zircon evaporation and K–Ar age determinations. Chem. Geol. 104, 75–92.

Whalen, J.B., Currie, K.L., Chappell, B.W., 1987. A-type granites: geochemical characteristics, discrimination and petrogenesis. Contrib. Mineral. Petrol. 95, 407–419.

Zaimen, F., 1994. Mise en évidence de plusieurs suites magmatiques dans la partie occidentale du terrain de Laouni (Hoggar, Algérie). Unpubl. PhD Thesis, Université de Paris-Sud, Orsay, 175 pp.

Zaimen, F., Black, R., Liégeois, J.P., Bonin, B, 1994. Âge cambrien du granite alcalin de Bahouinet N (Hoggar, Algérie). 15° RST, Nancy, abstr., 66.

Zheng, J.S., Mermet, J.F., Toutin-Morin, N., Hanes, J., Gondolo, A., Morin, R., Féraud, G., 1991. Datation $^{40}Ar/^{39}Ar$ du magmatisme et de filons minéralisés permiens en Provence orientale (France). Geodin. Acta 5, 203–215.

Ziegler, P.A., 1986. Geodynamic model for the Palaeozoic crustal consolidation of Western and Central Europe. Tectonophysics 126, 303–328.

Zorpi, M.J., Coulon, C., Orsini, J.B., Cocirta, C., 1989. Magma mingling, zoning and emplacement in calc-alkaline granitoid plutons. Tectonophysics 157, 315–329.